

Review

Mixer Design and Flow Rate as Critical Variables in Flow Chemistry Affecting the Outcome of a Chemical Reaction: A Review

Ilya V. Myachin and Leonid O. Kononov *

N.D. Zelinsky Institute of Organic Chemistry of the Russian Academy of Sciences, Leninsky Prospekt, 47, Moscow 119991, Russia

* Correspondence: kononov@ioc.ac.ru or leonid.kononov@gmail.com

Abstract: Flow chemistry offers several advantages for performing chemical reactions and has become an important area of research. It may seem that sufficient knowledge has already been acquired on this topic to understand how to choose the design of microreactor/micromixer and flow rate in order to achieve the desired outcome of a reaction. However, some experimental data are difficult to explain based on commonly accepted concepts of chemical reactivity and performance of microfluidic systems. In this mini review, we attempt to identify such data and offer a rational explanation of unusual results based on the suprameric approach. We demonstrate that variation in flow regime (determined by mixer design and flow rate) can either improve or worsen the reactivity and lead to completely different products, including stereoisomers. It is not necessary to mix the reagents with maximum efficiency. The real challenge is to mix reagents the *right way* since at a too high or too low flow rate (in the particular mixer), the molecules of reagents are incorrectly presented on the surface of supramers, leading to altered stereoselectivity, or form tight supramers, in which most of the molecules are located inside the suprameric core and are inaccessible for attack, leading to low yields.

Keywords: microfluidics; flow chemistry; mixer design; flow rate; mixing efficiency; supramers; supramolecular chirality; chemical reactions; glycosylation; stereoselectivity



Citation: Myachin, I.V.; Kononov, L.O. Mixer Design and Flow Rate as Critical Variables in Flow Chemistry Affecting the Outcome of a Chemical Reaction: A Review. *Inventions* **2023**, *8*, 128. <https://doi.org/10.3390/inventions8050128>

Academic Editors: Peng Du, Haibao Hu and Xiaopeng Chen

Received: 31 August 2023

Revised: 6 October 2023

Accepted: 10 October 2023

Published: 16 October 2023



Copyright: © 2023 by the authors. Licensee MDPI, Basel, Switzerland. This article is an open access article distributed under the terms and conditions of the Creative Commons Attribution (CC BY) license (<https://creativecommons.org/licenses/by/4.0/>).

1. Introduction

Over the past decades, chemistry in flow became a powerful tool of modern organic and inorganic chemistry, and many publications devoted to the study of chemical reactions in flow appeared. Dozens of reviews have been published on flow chemistry. Here, we mentioned only some of them [1–20], in which a reader can find further references on specific topics. The most comprehensive coverage and critical analysis of the recent flow chemistry accounts can be found in an outstanding review [11], in which an in-depth analysis of almost every aspect of performing chemical experiments in flow accompanied by invaluable advice on how one can control the reaction parameters to achieve the desired result is presented.

Flow chemistry (aka microfluidics [2]) offers several advantages for performing chemical reactions such as minimizing of accident risks and cheaper production of chemicals to name a few [7,11,13,17–19]:

- Flow chemistry facilitates the optimization of reactions at a much faster rate, resulting in a reduction in costs and time. Reaction time, temperature, ratio of reagents, concentration, and reagents themselves can all be rapidly modified. One reaction can be followed by another, separated by solvent, increasing throughput. Automated flow chemistry allows for rapid variation of reaction conditions on a very small scale ($\leq 100 \mu\text{L}$).

- Performing reactions in flow can be safer than in batch reactors, since only a small portion of reactive or hazardous material is transformed to product at any particular moment.
- The use of flow chemistry has the advantage of enhanced heat and mass transfer, which can result in faster reaction rates and higher yields.
- Flow reactors provide excellent reaction selectivity and allow for preparation of products that are not accessible under batch conditions.

Successful attempts to generalize the basic principles and fundamentals of flow chemistry [11] and to standardize the description of reactions in flow [14] have been advanced. Ten key issues in modern flow chemistry have been identified and discussed in detail [6]. Various designs of microreactors [3] and their classification [13] have been considered (for a more detailed discussion, *vide infra*). A state-of-the-art, future perspectives and challenges in creating reconfigurable microfluidic platforms, which would allow a user to easily tailor a microfluidic system for a specific application and “to tune a microscale experiment with the capacity to make real-time decisions”, has been reviewed [16].

There are many examples of the successful use of flow reactors for conducting reactions of various classes [1,11,13,15,18], including those useful for production of active pharmaceutical ingredients [17]. Functional group interconversion reactions have been successfully performed in continuous flow reactors [15]. Flow technology was found to be unexpectedly efficient in supramolecular chemistry [12,20]. A new paradigm for synthesis of natural products including carbohydrates has been proposed [4,5,9,10], which is based on performing traditional organic reactions under microfluidic conditions.

Among many parameters [11] the design of the microreactor/micromixer [11,21–25] and flow rate used are considered as the key factors that determine the outcome of a reaction performed in flow. One may think that sufficient knowledge has already been acquired [11] on this topic to understand how to select appropriate experimental conditions to achieve the desired reaction result.

However, only few researchers publish the “negative” results that could demonstrate their “inability” to forecast the result of a particular experiment; many researchers tend to modify the initial objectives of research after obtaining the positive results (“much of good science is opportunistic and revisionist”, as G. Whitesides put it [26]). For this understandable reason, reports of detailed studies of the influence of the design of the microreactor/micromixer and/or flow rate on the outcome of the real-life reactions (as opposed to the studies of “test reactions” in flow, *vide infra*), performed by practicing organic chemists (rather than by experts in chemical engineering), are rare. Conditions for successful practically important chemical transformations in flow are mostly reported.

This situation creates a “research gap” between reports on successes or failures of reactions, performed under specific conditions in flow, and understanding the reasons lying behind. Moreover, some experimental data are difficult to explain based on commonly accepted concepts of chemical reactivity (in general) and performance of microfluidic systems (in particular). In this mini review, we attempt to identify such data and offer a rational explanation of unusual results based on the supramer approach (*vide infra*) [27].

2. Mixing Performance

Typical microfluidic systems are featured by low Reynolds numbers (Re , [28]) ($Re \leq 1000$ [1,8,29]) that would generally suggest a laminar flow, even in reactors in which biphasic reactions proceed [30], and guarantee that there is no turbulence and therefore no back-mixing in the reactor [8]. This notion may create the wrong impression that mass transfer of reactants in microfluidic systems is controlled by diffusion only; in fact, convection/advection can also contribute significantly to the mass transfer in these systems (*vide infra*).

It is clear, even from general considerations, that the reagents need to be mixed well for the effective reaction to occur [29,31–37]. This review is limited to discussion of passive [29,35,36] mixing that does not rely on external energy input. This mixing is

realized within mixing devices (micromixers), which often serve also as microreactors (for this reason, hereinafter we denote them as “microreactors/micromixers”).

Many studies [21,29,35–92] were dedicated to modeling various types of micromixers/microreactors and determining their mixing efficiency (mixing quality) theoretically and/or experimentally using a set of test reactions [39,57,63]. This widely used “chemical” approach for accessing the mixing efficiency, unlike purely physical approaches like flow imaging, is based on the *implicit supposition* that the dependence of outcome of a chemical reaction, performed in flow, on mixing conditions is determined by mixing efficiency of the micromixer/microreactor used. We emphasize that most experimental studies of mixing efficiency of different micromixers/microreactors are in fact providing information on chemical reactivity in the reactions performed under flow conditions using these micromixers/microreactors. This means that the observed dependence of conversion of the starting compound and product yield on mixing conditions may reflect not only the mixing issues (as usually believed) but also the influence of other (unknown) factors that are affected by changing the mixing mode. This opens the way for alternative views on chemical reactivity as exemplified by application of the supramer approach [27] to the flow chemistry (*vide infra*).

The mixing performance of different types of mixers has been previously compared [21, 35,36,43,53,57,69,70,72,79,93]. The main message for the practicing synthetic chemist from these studies is that the mixing quality is controlled by the flow regime in the mixing device. Importantly, the flow regimes may differ considerably for different mixers; for the same mixer flow regimes may also vary depending on the flow rate (an example is shown in Figure 1).

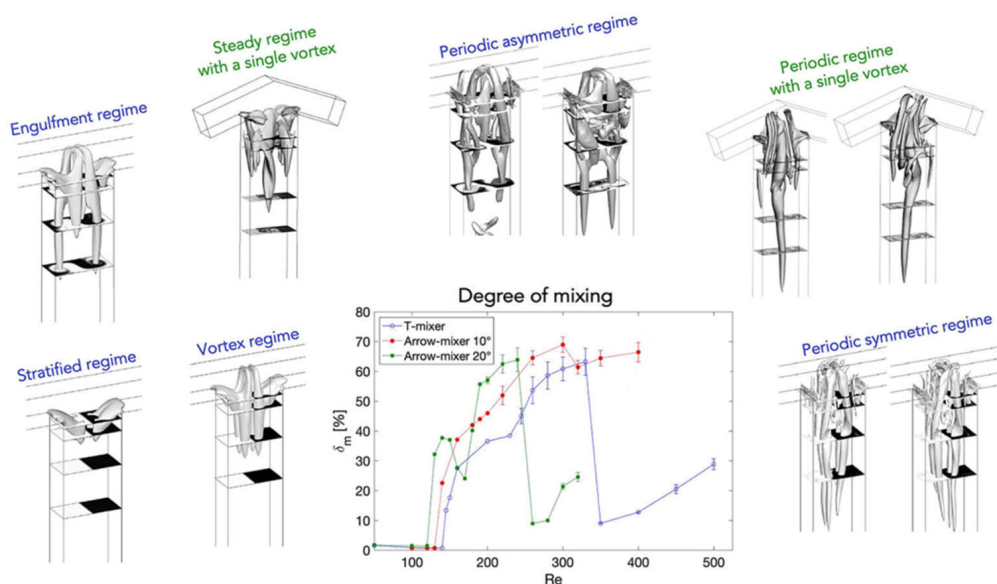


Figure 1. Summary of the steady flow regimes and mixing quality (δ) as a function of the Reynolds number (Re) in T-shaped and arrow-shaped micromixers. Adapted with permission from [79].

In most studies mainly the Reynolds number was used to describe the flow regime (but occasionally other numbers were used [94]). However, the Reynolds number alone is not necessarily always trustworthy for estimating mixing quality in micromixers/microreactors. It was demonstrated that mixing quality of a simple and widely used T-shaped micromixer sharply increases in the “engulfment flow regime”, featured by the increased vorticity (Figure 2) hence mixing quality, which occurs at the high flow rates even in the low Reynolds number range ($Re \sim 200$) (Figure 3) [43]. It was concluded that the Reynolds number is not suitable for identification of the flow regime, since it varies a lot for different mixer geometries under similar flow regimes [43].

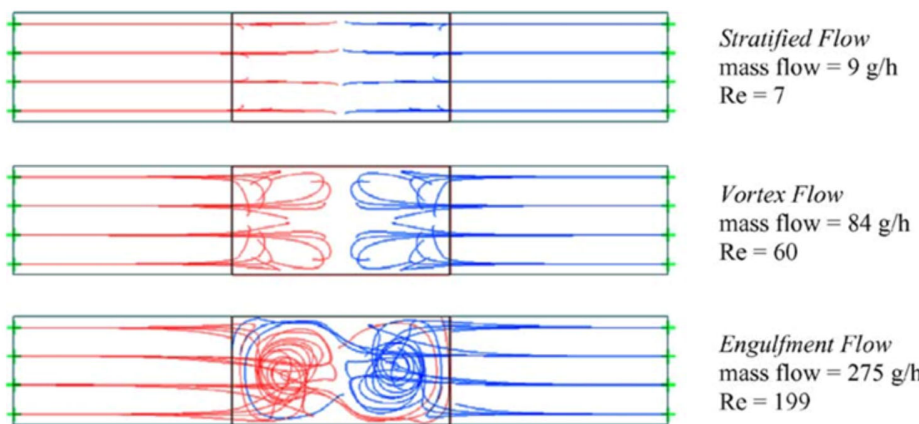


Figure 2. Streamlines inside a T-shaped micromixer (channel widths 300 and 600 μm) at different mass flows. View is into the mixing channel (left (red) and right (blue) are the inlet channels). Reproduced from [43] with permission from Elsevier.

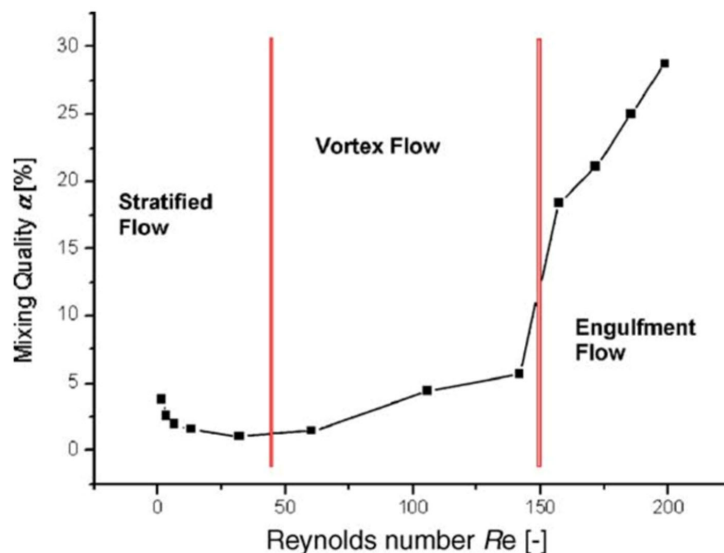


Figure 3. Mixing quality (α) over the Reynolds number (Re) for a T-shaped micromixer. Reproduced from [43] with permission from Elsevier.

Using examples of micromixers/microreactors of varying complexity (from the most studied simple T-shaped micromixers [35,43,44,46,48,49,53,58,60,69,70,72,74,76,79–85,88,91] to more sophisticated “split-and-recombine” microreactors [35–37,47,51,70,91,95,96]), it was shown that regardless of the value of the Reynolds number, mixing can be effective at least in some flow regimes. Especially effective is the so called “chaotic mixing/advection” [3, 29,31,42,96]. Operation conditions of passive mixers based on chaotic advection can be distributed around the characteristic lines in the Pe – Re diagram for a wide range of Reynolds numbers (see Figure 4). Importantly, the passive micromixers work well either at low Reynolds numbers and low Peclet numbers (bottom left corner in Figure 4) or at high Reynolds numbers in the transition regime to turbulence (top right corner in Figure 4). Noteworthy, chaotic micromixers can be designed for use in a wide range of Reynolds numbers. Importantly, mixing with chaotic advection does not depend on the Péclet number [29].

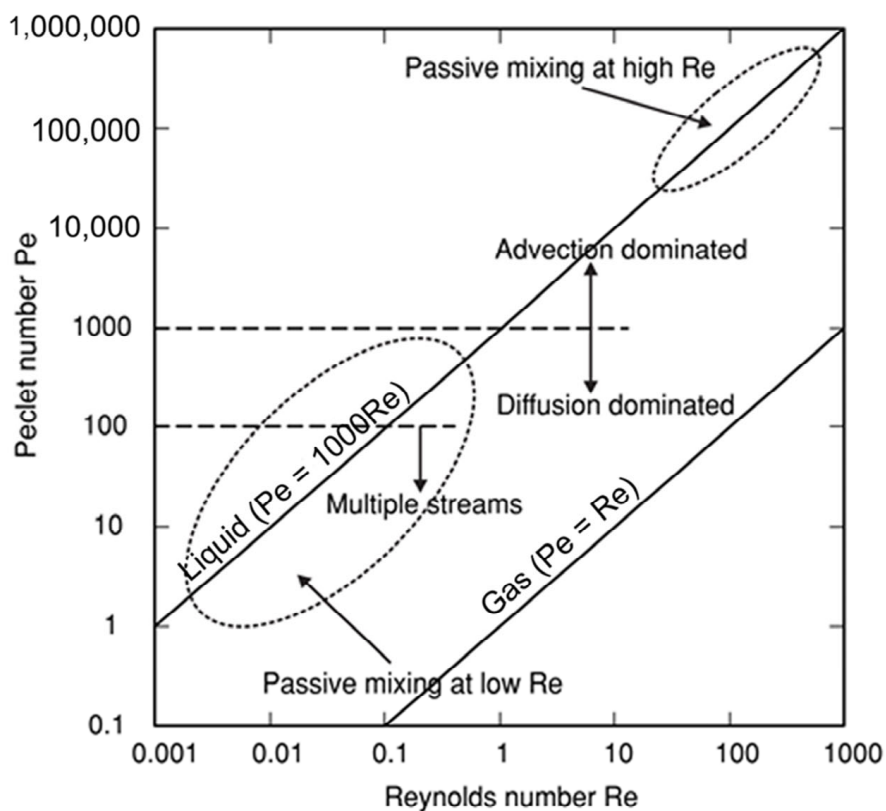


Figure 4. The Pe - Re diagram. The Reynolds number (Re) describes the flow regime in the mixing channel (Re is a convenient parameter for predicting whether a flow regime will be laminar or turbulent), while the Péclet number (Pe) represents the ratio between convection/advection and diffusion (when $Pe \ll 1$, then diffusive effects dominate over convective/advective transport, whilst the opposite is generally true for $Pe \gg 1$). Adapted with permission from [29]. © IOP Publishing. All rights reserved.

Among many different micromixers designed for microflow systems, a Comet X-01 micromixer should be highlighted. This mixer has previously been used to perform and optimize various reactions [4,97–114]. Inside this mixer, the flow is split into three and merged back into one (repeated five times) (see Figure 5 and supporting information file for Ref. [113]) remotely resembling that in the previously mentioned “split-and-recombine” microreactor [35–37,47,51,70,91,95,96]) featured by “chaotic mixing” [3,29,31,42,96], which ensures efficient mixing regardless of the Reynolds number [3]. The unique design of the Comet X-01 micromixer made possible the discovery of unprecedented results described later in this review (*vide infra*).

Concluding this section, we must stress that current knowledge suggests the importance of mixing issues in chemical reactions to be related to the relative values of the mixing times as compared to the reaction times. For a detailed discussion and recommendations for choosing the design of the commercially available micromixers suitable for specific applications see [57].

The effects of mixing on the outcome of the sufficiently slow chemical reaction performed in flow can usually be neglected. If the reaction time is significantly longer than the mixing time, it can be considered that the reaction takes place under homogeneous environment (“homogeneous concentration field”). In such a situation, enhancing the mixing performance cannot increase the conversion rate [57].

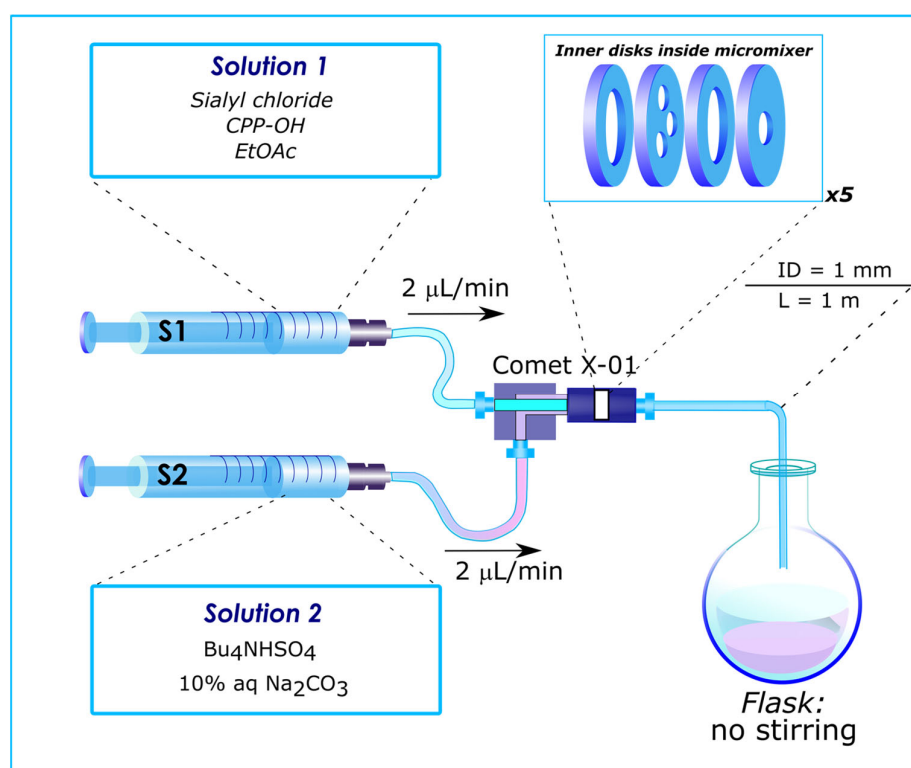


Figure 5. Flow reactor, based on Comet X-01 micromixer, used for glycosylation experiments. S1, S2—syringes. Internal volume of Comet X-01 micromixer—0.1 mL, that of outlet capillary—0.785 mL. Reproduced with permission from [114].

At the same time, fast and ultrafast reactions (as compared to mixing of reagents) should be extremely sensitive to changes in mixing efficiency which is determined by the flow regime realized in the mixer of specific design at the indicated flow rate. In this situation “the reaction takes place in a heterogeneous concentration field with multilamellae structures which are determined by the mixing process. The length scales of these structures as well as the time scale of their generation can have a strong influence on the conversion rate. In the case of a reaction system with competitive parallel or consecutive reactions, mixing time can also affect the selectivity of this system, especially if parallel reactions proceed at a different time scale” [57].

For this reason, many studies report the influence of both parameters (mixer design and the flow rate) on the reaction outcome, and they will be discussed together in the next section. Note that until recently, most of the reports on flow chemistry dealt with conversion of the starting material and product(s) yield as measures of the reaction progress. Issues of stereoselective formation of stereoisomers were mainly neglected; the rare examples will be mentioned below.

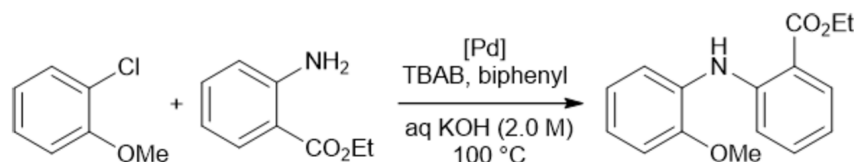
3. Influence of Mixer Design and Flow Rate on Reaction Outcome

The flow rate plays an important role in flow reactions. There is a lot of evidence that flow rate can influence the reaction yield. There are cases when the yield increases both with a decrease [110,115] and with an increase [116–119] in the flow rate.

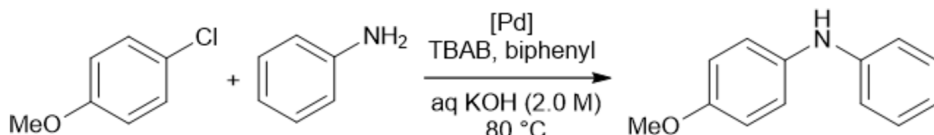
A change of flow rate with constant path length after mixing expectedly results in the change of reagents residence time (*vide infra*). A decrease in flow rate usually leads to an increase in product yield due to increase in residence time. However, in some cases due to increased residence time, the number of side processes leading to formation of undesirable products may also increase leading to a decrease in the yield of the target product. There are situations in which an increase in the flow rate (hence, the Reynolds number) leads to an increase in product yield [113]. However, increasing the flow rate is not a panacea: if the

flow rate is too high, then the reactants simply will not have enough time to react inside the reactor. It is generally accepted that for the optimal course of the reaction, it is necessary to find a golden mean between these extremes.

The crucial role of mixing efficiency, determined by the mixer design (*vide supra*), for chemical reactions performed under flow conditions was demonstrated for C–N cross-coupling reactions (Schemes 1 and 2) [120]. In one case, the capillary reactor contained grains around which the reaction solutions flow. In this case, in the thin films formed between the grains, mixing occurs efficiently, and the reaction is complete within 6 min. In another case, there was a free capillary in which conditions for effective mixing were not created. As a result, the yield after the same time was relatively small (Figure 6).



Scheme 1. Palladium-catalyzed C–N cross-coupling reaction performed in flow with packed bed and open tube reactor (see Figure 6) [120].



Scheme 2. C–N cross-coupling palladium-catalyzed reaction performed in flow with various packed bed volumes (see Figure 7) [120].

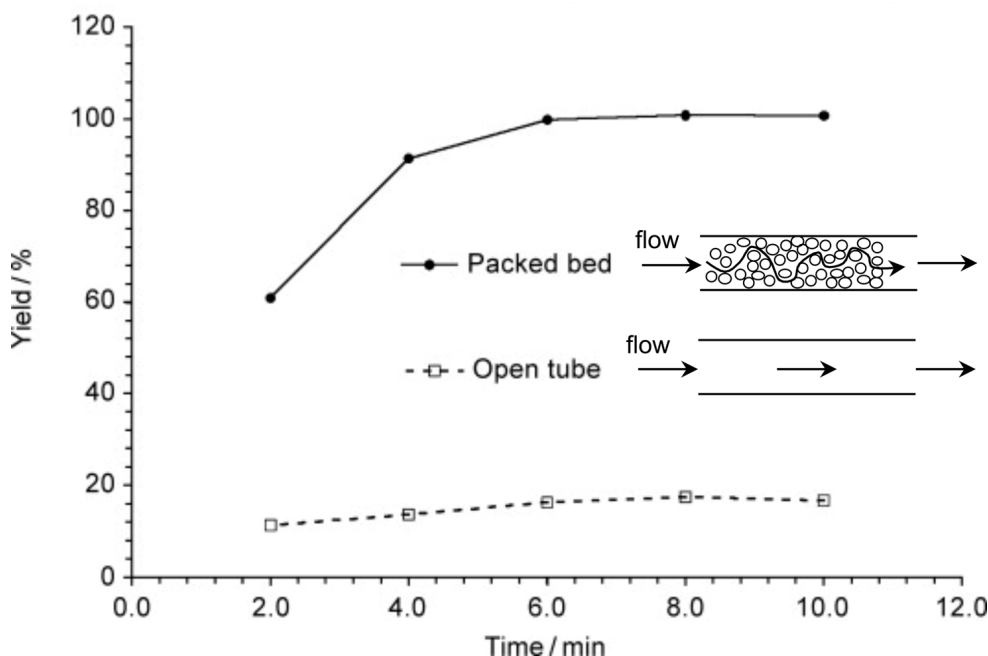


Figure 6. An example of the crucial role of mixing efficiency: the reaction (see Scheme 1) proceeds in high yield only when packed bed capillary is used for mixing reagents. Time indicated designates the residence time. Adapted with permission from [120]. Copyright © 2010 WILEY-VCH Verlag GmbH & Co. KGaA, Weinheim.

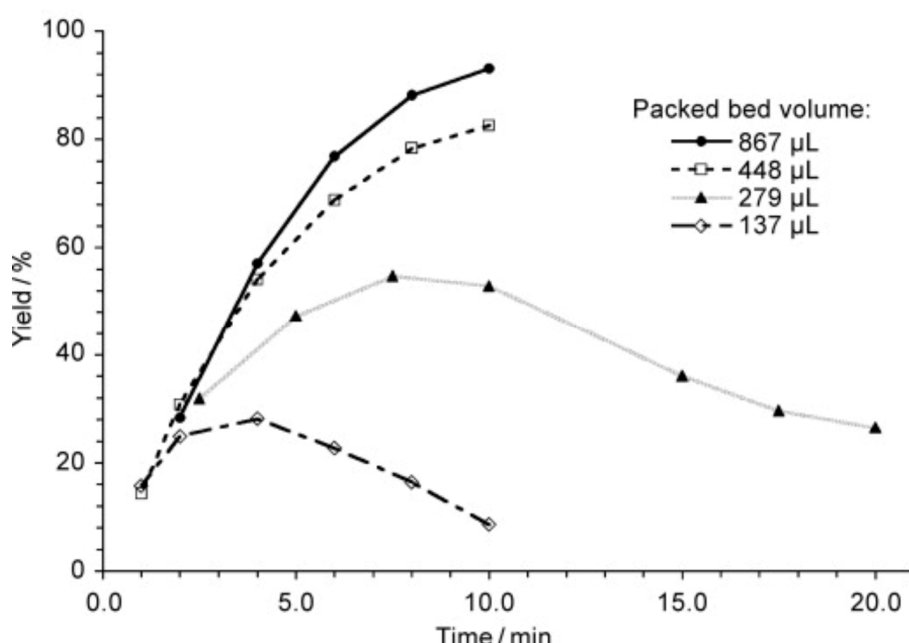
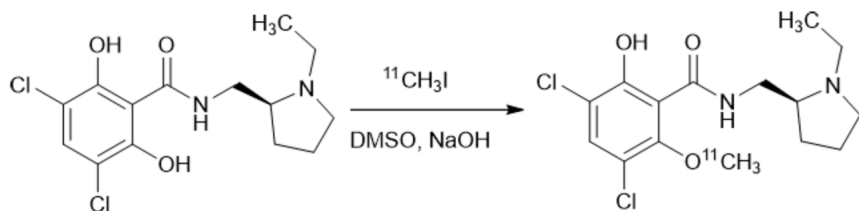


Figure 7. Comparison of the packed beds differing in size: the reaction (see Scheme 2) proceeds in high yield if the large packed bed capillary is used for the reaction proceeds (see also Figure 6). Time indicated designates the residence time. Adapted with permission from [120]. Copyright © 2010 WILEY-VCH Verlag GmbH & Co. KGaA, Weinheim.

More than that, a study of a similar reaction [120] showed that the yield depends on packed bed volume (Scheme 2, Figure 7). When the size of the packed bed was decreased, the yield of the reaction was decreased too. Note the maxima on the plots of the yield against the residence time. Since it was demonstrated that the product was not degrading over time the authors attributed the decrease in yield to changes in mixing performance at low flow rates (larger residence time).

An increase in the mixing efficiency often leads to an improvement of the reaction outcome. A remarkable example is the preparation of [¹¹C]raclopride under flow conditions by the methylation reaction (Scheme 3) [121]. During the study of the impact of the micromixer/microreactor design on this process, mixers with a consistently increasing number of additional loops (Figure 8a–c) were used, which were expected to increase the mixing efficiency and improve the reaction outcome. It was shown that reaction with non-radioactive CH₃I resulted in higher yields in the “abacus” micromixer than in the “no loop” micromixer (5.8% and 1.3% yields, respectively). At the stage of using radioactive ¹¹CH₃I as the methylation reagent it was also shown that the “full loop” microreactor is better than the “abacus” micromixer (relative radioactivity 25.6 and 16.0, respectively).



Scheme 3. Alkylation reaction performed in various types of flow reactors (see Figure 8) [121].

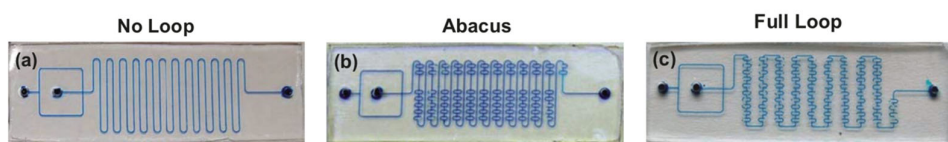


Figure 8. Three micromixers used for performing alkylation reaction (see Scheme 3) featured by different mixing efficiency. (a)—simple channel micromixer without additional loops (“no loop”); (b)—abacus-like micromixer with some additional loops (“abacus”); (c)—micromixer with maximum additional loops (“full loop”). Adapted with permission from [121].

The outcome of two-phase reactions carried out in flow may also depend strongly on the mixing method. This was shown using a Heck reaction where two modes of oxygen delivery to the reaction solution were compared (Figure 9) [122]. The main idea of this design is that the flows of liquid and gas occur not in one capillary, but in two parallel ones (Figure 9a). This can be achieved using the setup shown in Figure 9b: two parallel capillaries are separated by the PDMS membrane. This setup allows one to adjust the flow rate for each phase independently. Dual-channel design compared to slug flow showed higher convenience and higher yields: $\geq 75\%$ in dual-channel and $\leq 65\%$ in mono-channel modes (^1H NMR data).

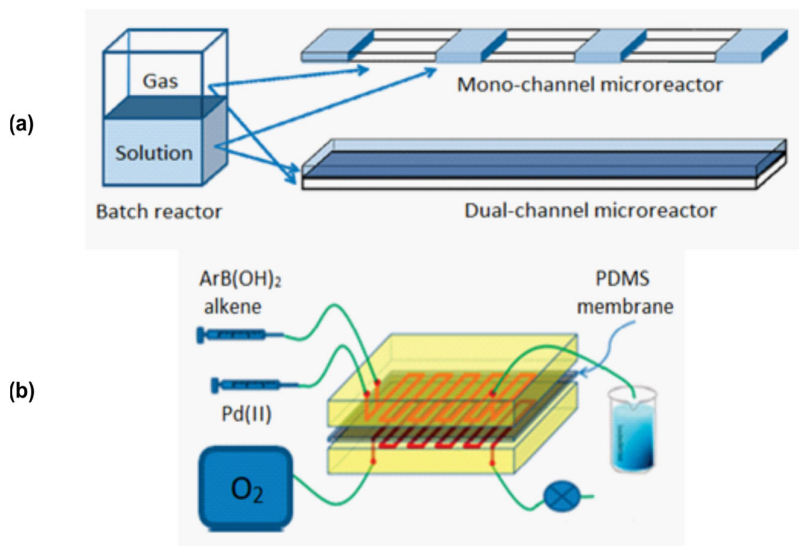


Figure 9. Mixer design for performing oxidation reaction under flow conditions. (a)—illustration of various modes of contact area between gas and liquid phases; (b)—schematic illustration of the dual-channel system. Adapted with permission from [122].

The mixing efficiency of a T-shaped micromixer is known to strongly depend on the flow rate [57]. When such mixer was used for a study of efficiency of metalation of substituted bromobenzenes with butyl lithium followed by quenching with methanol (Figure 10a) the inflection points on the plots of the yields of both electron-rich and electron-poor compounds were observed at 14 mL/min flow rate suggesting that the increased mixing efficiency within the T-shaped micromixer at a high flow rate, hence higher product yield, is due to a change in the flow regime [118] (Figure 10b; compare with Figure 3).

The design of the mixer plays an important role in the processes, during which further transformation of the product as a result of side reactions is possible. This is well illustrated by the Friedel–Crafts reaction (Scheme 4) [123]. In this example, sequential alkylation of the aromatic system occurs. The monosubstituted (main) and disubstituted (side) products were obtained in different ratios when different micromixers were used for mixing reagents. In a simple T-shaped micromixer the yields of the main and the side products were 36% and 31%, respectively. When the YM-1 mixer [45] was used the yields of the main and the

side products became 50% and 14%, respectively. The best result was achieved in the IMM mixer [21,35]: the yields of the main and the side products were 92% and 4%, respectively.

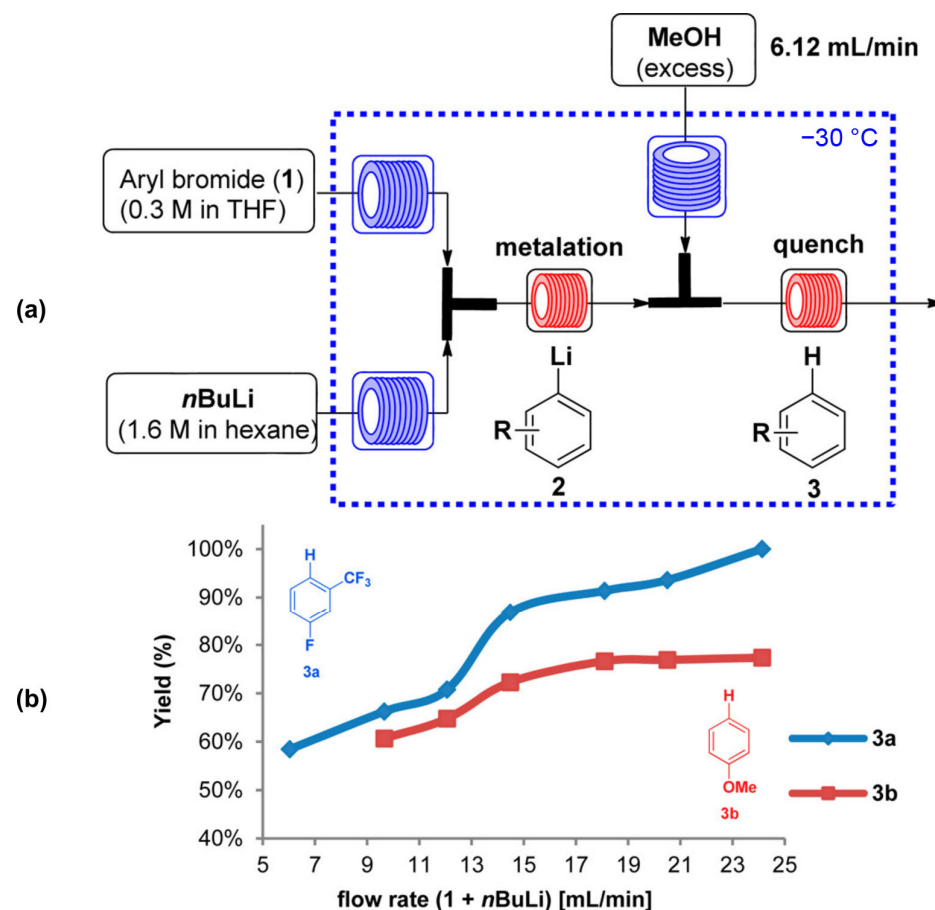
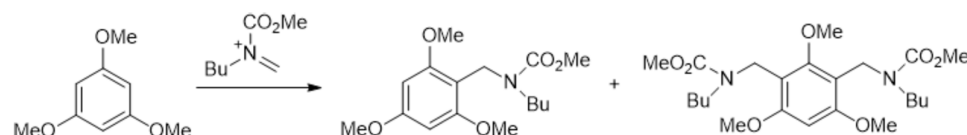


Figure 10. Investigation of mixing performance for the metalation step as a function of flow rate of aryl bromide (**1**) and *n*-BuLi: (a)—schematic illustration of the flow system. (b)—the yield of **3** as a function of the total flow rate. Adapted with permission from [118]. Copyright 2016 American Chemical Society.



Scheme 4. Friedel–Crafts reaction performed in flow using three types of micromixers: T-shaped, YM-1, and IMM [123].

Such a strong influence of the mixer design (hence the mixing efficiency) was explained [123] from the point of view of the model proposed by Rys [124] (see also a discussion in [57] on competitive consecutive reactions). This model can be used to describe multistep rapid reactions whose rate is limited by the diffusion of reagents (Figure 11). At the first time interval after mixing, regions with an increased concentration of reagent molecules (**B**) surrounded by a solution of another reagent (**A**) are formed. At the points of contact, the first product (**P1**) is formed, which, without effective mixing, does not have time to diffuse into the outer sphere and continues to react to give **P2** at the further time interval.

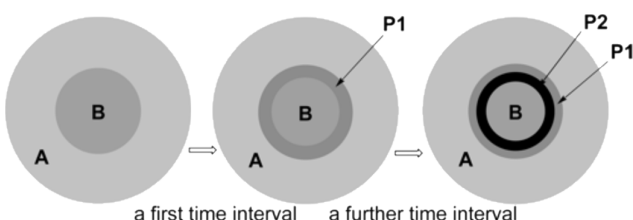


Figure 11. A model [124] of the course of a liquid two-step reaction (like in Scheme 4) where diffusion of reagents is main limitation of reaction rate. **A, B**—initial reagents, **P1**—monosubstituted product, **P2**—disubstituted product. Adapted with permission from [123].

During a study of Lewis acid (TMSOTf) promoted microfluidic glycosylation of a 4,6-galactose diol with a 5-azido-sialyl imidate in EtCN at $-78\text{ }^{\circ}\text{C}$ (bath temperature) a noticeable influence of the mixer design on the outcome of glycosylation was detected for the first time [100]. Both employed micromixers (IMM and Comet X-01) allowed highly efficient synthesis of the target disaccharide (yields were virtually quantitative in both cases). However, stereoselectivity was higher when the IMM micromixer was used ($\alpha/\beta = 95:5$) as compared to stereoselectivity achieved in glycosylation with the Comet X-01 micromixer ($\alpha/\beta = 88:12$). The authors explained this difference in selectivity by higher temperature in the second case, leading to lower stereoselectivity, “probably due to poorer heat removal of Comet X-01” (the reaction is exothermic) [100].

The influence of the mixer design on the result of glycosylation was also observed in the sialylation reaction of a substituted phenol (Scheme 5) performed at room temperature under conditions of phase transfer catalysis [113,114]. Here, two different micromixers were used: a Comet X-01 micromixer (*vide supra*), where flow splits into three and joins together several times (see Figure 5), and a simple T-shaped micromixer. At $2\text{ }\mu\text{L}/\text{min}$ flow rate the product yields in both cases turned out to be similar: 36% and 33%, respectively. However, the difference in stereoselectivity (α/β) was more significant: 6.2:1 and 13.3:1, respectively. Note that the same reaction performed in batch is stereospecific providing a kinetically controlled α -isomer as the only product of glycosylation [113].



Scheme 5. Sialylation reaction under phase transfer conditions performed in flow. CPP-OH—4-(3-chloropropoxy)phenol [113,114].

The effect of the flow rate on the yield and on the stereoselectivity of glycosylation was observed in this sialylation reaction (Scheme 5) [113]. In this case, with the increase of the flow rate from 2 to $250\text{ }\mu\text{L}/\text{min}$, the yield and stereoselectivity decreased from 36% to 11% and from $\alpha/\beta = 6.2:1$ to $\alpha/\beta = 1.9:1$, respectively. However, after further increase of the flow rate to $1000\text{ }\mu\text{L}/\text{min}$ the yield and stereoselectivity increased to 37% and $\alpha/\beta = 3.8:1$, respectively. Therefore, both high ($1000\text{ }\mu\text{L}/\text{min}$) and low ($2\text{ }\mu\text{L}/\text{min}$) flow rates result in similar yields and stereoselectivities, but intermediate flow rates give worse results. The influence of flow rate and mixer design on the product yield could be easily rationalized within the framework of the mixing-centered concept, discussed above, which emphasizes the importance of the adequate flow regime for efficient mixing of reagents.

However, the unexpected loss of stereoselectivity under microfluidic conditions and its dramatic dependence on mixing conditions (mixer design and flow rate), hence flow regime, does not fit the current knowledge [125–128] on the origin of stereoselectivity of glycosylation. It is unclear how flow rate or mixer design could affect the stereoselectivity of reactions that involve “isolated” molecules.

However, the found phenomenon can be rationally discussed within the framework of supramer hypothesis (supramer approach) [27], according to which the real reacting species in many cases are supramolecular aggregates (supramers) rather than single molecules of reacting substances (the “molecular species”). Recent studies revealed [129–137] that even macroscopically homogeneous aqueous and non-aqueous solutions of low-molecular-mass non-amphiphilic compounds can contain nano- and mesoscale heterogeneities (size from ca. 1 nm to 10^2 – 10^3 nm) that are kinetically stable, although very small interaction energy, which does not exceed $k_B T$ [138], is involved. The most probable reason for their existence and omnipresence is the “solvophobicity-driven mesoscale” structuring [136] promoted by even minute amounts of “solvophobic admixtures” [27,136] that are present in most commercially available compounds [133] since “no truly pure chemicals exist” [136].

Considering the presence of such heterogeneities, supramers in our terminology [27], which belong to the realm of soft matter, we have been developing the supramer approach (*vide supra*) for the description of chemical reactions (see Refs. [27,139–141] and references cited therein). According to the supramer approach, the “presentation” (spatial orientation) of molecules on the surface of supramers of glycosyl donor (or glycosyl cation formed from it) may play an important role in determining reaction stereoselectivity (see Figure 12).

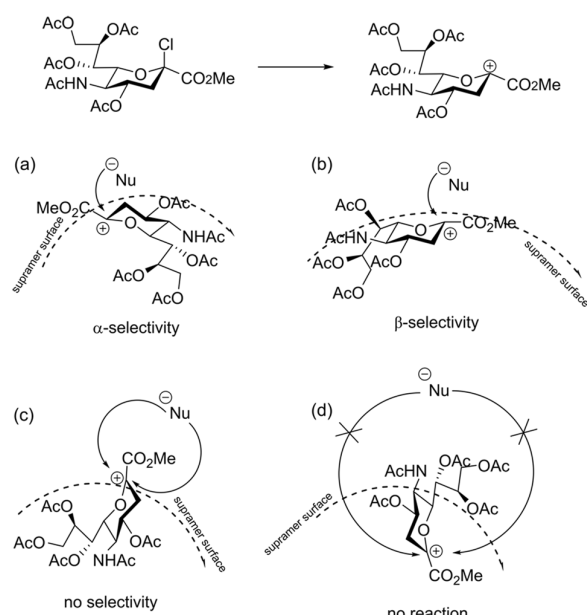


Figure 12. Presentation of glycosyl cation on supramer surface: (a,b)— α - and β -selective reactions, respectively, (c)—nonselective reaction, (d)—no reaction. Adapted with permission from [114].

The first stage of the reaction is formation of glycosyl cation which next reacts with nucleophile (Figure 12). Apparently, this stage is the most important one, since the presentation of the glycosyl cation on the surface of the supramer would determine the face of the glycosyl cation on which the nucleophile attack will occur leading to different stereoisomers of the product (Figure 12a–c). It is also possible that the cationic center is hidden inside the supramer (Figure 12d), which would prevent the attack of the nucleophile and lead to a decrease in reactivity of the starting compound (lowering conversion) and the product yield. Similar processes of orientation of molecules on a surface apparently occur during the formation of J-aggregates [142–147] for which the dependence of the resulting types of aggregates on the mixing method was established [148,149].

According to the explanation suggested [113], the efficiency of disaggregation/rearrangement (see Figure 13) of sialyl chloride supramers [27] varies under different mixing modes (in particular, at different flow rates). This makes the S_N1 -like pathway within S_N1 – S_N2 -continuum of glycosylation mechanisms [150,151] possible under microfluidic conditions, leading to formation of both anomers of CPP sialoside (Scheme 5).

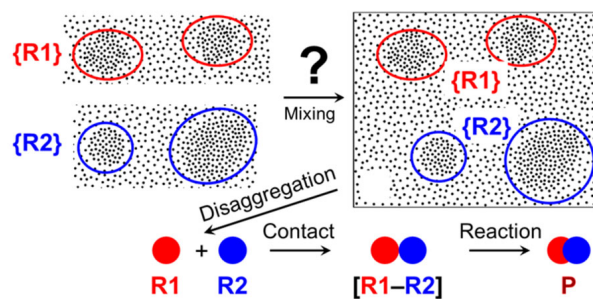


Figure 13. Reagent molecules inside solution domains (supramers) **[R1]** and **[R2]** cannot react with each other. Efficient destruction of domains is required for all molecules of reagents **R1** and **R2** to react—a clue for increasing reactivity of reagents and achieving high yield of product **P**. Supramers may react on their surfaces, in this case asymmetric environment of the surface molecules (presentation, see Figure 12) may lead to stereoselective reactions. Reproduced from [27] with permission from the Royal Society of Chemistry.

According to the authors [113,114], the β -anomer is formed only if sialyl chloride supramers undergo disaggregation (Figure 14), which seems to be more effective in Comet X-01 micromixer (apparently featured by “chaotic mixing” [3,29,31,42,96]) than in T-shaped micromixer. This result suggests that high efficiency of mixing is not a panacea for improving the reaction outcome.

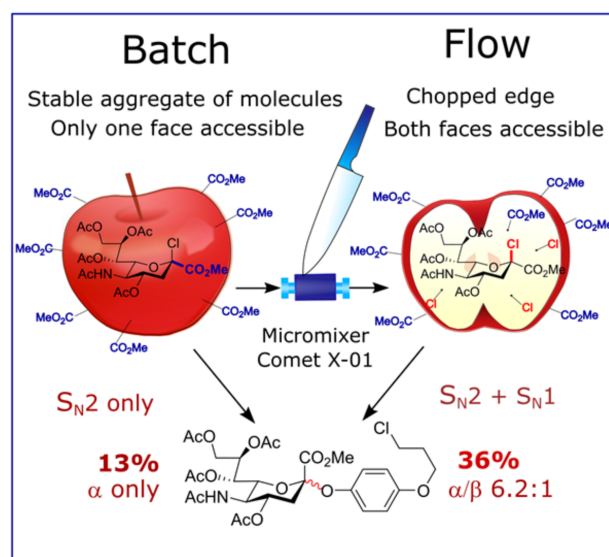


Figure 14. A model of supramers of sialyl chloride in the reaction mixture. In batch reactor the supramers are visualized as a whole intact “apple” (left panel). The spatial orientation of molecules of sialyl chloride in such supramers (presentation, see Figure 12) allows glycosylation from only one face within S_N2 -like pathway leading to formation of only α -isomer. During “efficient mixing” of reaction mixture in Comet X-01 micromixer (**M**) the “apple” is chopped allowing the molecules of sialyl chloride to show *both* faces on the edge of the apple allowing S_N1 -like mechanism which leads to formation of both α - and β -isomers (right panel). Reproduced with permission from [113]. Copyright © 2022 WILEY-VCH Verlag GmbH & Co. KGaA, Weinheim.

We must emphasize that this is the first documented example [113,114] of the influence of flow regime on stereoselectivity of a chemical reaction (that does not involve epimerization of the product), which has additionally been rationally explained.

An increase in the *syn/anti* ratio (from 8:1 to 18:1) of the product upon increase in the flow rate has been reported for organocatalyzed 1,4-addition of aldehydes to nitroolefins. The authors explained this by epimerization of the product by the catalyst, which be-

comes more profound at increased residence times that inevitably accompany lower flow rates [152].

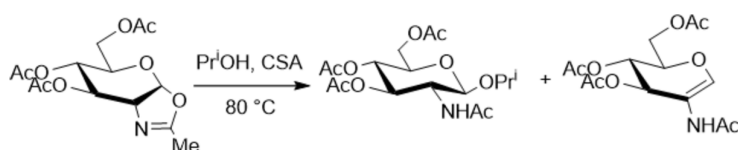
Continuous telescoped two-carbon homologation of esters to α,β -unsaturated esters was performed under microfluidic conditions, which incorporated an ester reduction, phosphonate deprotonation, and Horner–Wadsworth–Emmons olefination into a single, uninterrupted system. The authors are puzzled by the fact that the *E/Z* selectivity of the olefination in flow was noticeably higher than that under batch conditions using similar reagents [153].

All other previous studies of reactive mixing (see, e.g., [39,57,63]) were concerned with conversion of the starting compound and product yield as the measure of mixing quality. It is difficult to surmise from basic chemical principles [154] that flow regime could alter stereoselectivity of glycosylation, which is considered to be governed (for kinetically controlled reactions, to which glycosylation belongs) by relative rates of reagent attack on *Re*- and *Si*-faces of glycosyl cation, a real glycosylating agent in these systems [114]. One can speculate that the breakdown of symmetry (leading to inequality of these rates) could occur in the presence of an external chiral stimulus. Note that vortex-controlled generation of supramolecular chirality has been documented for batch systems [148,149,155–157].

The recently discovered [20] phenomenon of enhanced formation of non-covalent bonds under flow conditions, thus easing the self-assembly of new supramolecular structures, might also be related to rearrangements of supramers of reactants induced by shear stress in flow as discussed above (see Figure 14). Specifically, we hypothesize that supramers of reactants disaggregate (partially or completely) (see Figures 13 and 14) under flow conditions in a dynamical fashion creating the fragmented supramers (and, ultimately, the “molecular species”) that are (1) more reactive compared to the parent supramers, present in the starting solutions, and (2) capable of forming supramolecular architectures different from those formed “passively” [20] in the flask from the parent supramers. In line with the discussion above, we propose that the ease of supramolecular assembly in flow would dramatically depend on the flow regime, hence on the mixer design and the flow rate used.

Similar reasoning might explain the well-known phenomenon of decreasing the reaction time in flow as compared to that of the same reaction performed in batch. From the supramer point of view, shear stress in flow might induce fragmentation of the parent supramers, which exist in solution before the reaction, leading to formation of more reactive species and making the reaction faster. Traditional explanation of this considerable decrease in reaction time (e.g., from 24 h in batch to 7 min in flow [152]) would involve listing beneficial features of the microfluidic technique such as improved mass transfer due to efficient mixing, fast heat transfer, and residence time control to name a few (see, e.g., [5,18,19]).

The design of the mixer and flow rate can strongly determine the reactivity of a substance. This phenomenon was demonstrated using glycosylation of isopropyl alcohol with oxazoline as the glycosyl donor (Scheme 6) carried out in a Comet X-01 micromixer (Figure 15) [110]. As expected, at high flow rates, the yields of both products were low—the reaction did not have enough time to occur. With a decrease in the flow rate, the yields expectedly increased. But at some point, at very low flow rates (flow rate $\leq 43 \mu\text{L}/\text{h}$), the acid-labile oxazoline stopped reacting and the starting reagents were recovered. This apparent loss of reactivity was observed *only* when Comet X-01 micromixer was used. However, when a Comet X-01 micromixer was replaced with a T-shaped micromixer (at 30 $\mu\text{L}/\text{h}$ flow rate), the expected reaction products, glycoside and glycal, appeared in the reaction mixture. Thus, the change in mixer design (from Comet X-01 micromixer to T-shaped micromixer) apparently altered the flow regime resulting in better mixing of reagents, if we follow the mixing-centered concept, discussed above.



Scheme 6. Glycosylation reaction of isopropyl alcohol by glyco-oxazoline. CSA—camphorsulfonic acid.

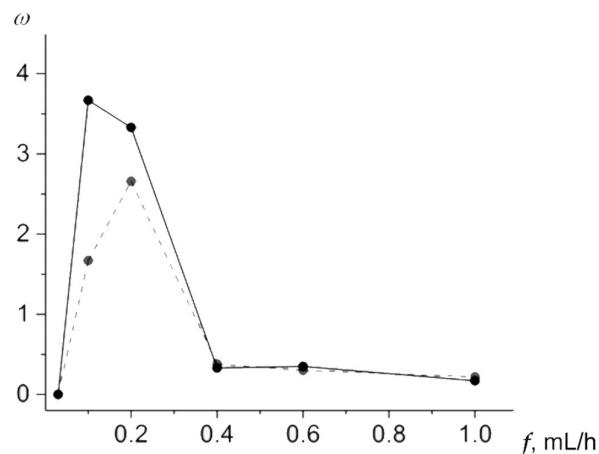


Figure 15. Formation of products in glycosylation reaction performed in flow at different flow rates (Scheme 6) using Comet X-01 micromixer. Relative amounts (ω) of products: dashed line—isopropyl glycoside, solid line—glycal (side product). f —flow rate, mL/h. No reaction was observed at low flow rates ($\leq 43 \mu\text{L}/\text{h}$). Adapted with permission from [110]. Copyright (2019), Springer Nature.

However, within the framework of the supramer approach [27] (*vide supra*), this result apparently suggests a higher disaggregation of the supramers of reagents under these conditions (using a T-shaped micromixer), which allows the chemical reaction between them to occur. Apparently, at very low flow rates ($30 \mu\text{L}/\text{h}$) in the Comet X-01 micromixer, the molecules of this glycosyl donor are located inside the core of tight supramers (similar to those discovered recently [113,114,139,158]) or presented on the surface of supramers in such a way that the anomeric position becomes inaccessible for attack (which is manifested as an enhanced stability of oxazoline under the action of acid), similarly to the situation shown in Figure 12 for glycosyl cation derived from sialyl chloride. Based on these facts, we conclude that the flow rate in combination with change in the mixer design in this case directly affects the *reactivity* of molecules probably by changing the flow regime which makes disaggregation (see Figures 13 and 14) of the supramers of reagents (im)possible thus altering the observed reactivity pattern.

Similar observations were made earlier for another reaction [159], where it has been proposed that the observed decrease in conversion at low flow rates is related to the change in the flow regime from “dispersed flow regime” (good mixing) to “stratified flow regime” (bad mixing) (Figure 16) supported by mixing experiments with non-reacting substances. Indeed, this phenomenon of “the dependence of mass transfer on the two-phase flow patterns” was studied in single- and two-phase flow systems [61,64]. However, as in the previous example, one can speculate that a change in the flow rate leads to a change in the flow regime, which modulates the efficiency of disaggregation of the supramers of reagents. As a result, at low flow rates, some of the molecules are located inside the core of tight supramers [113,114,139,158] and cannot react. As the flow rate increases, the efficiency of disaggregation increases, and the conversion rate increases accordingly. With a further increase in the flow rate, the conversion decreases, which may be due either to insufficient contact time of the reagents or to generation of supramers of different type formed during disaggregation of the parent supramers.

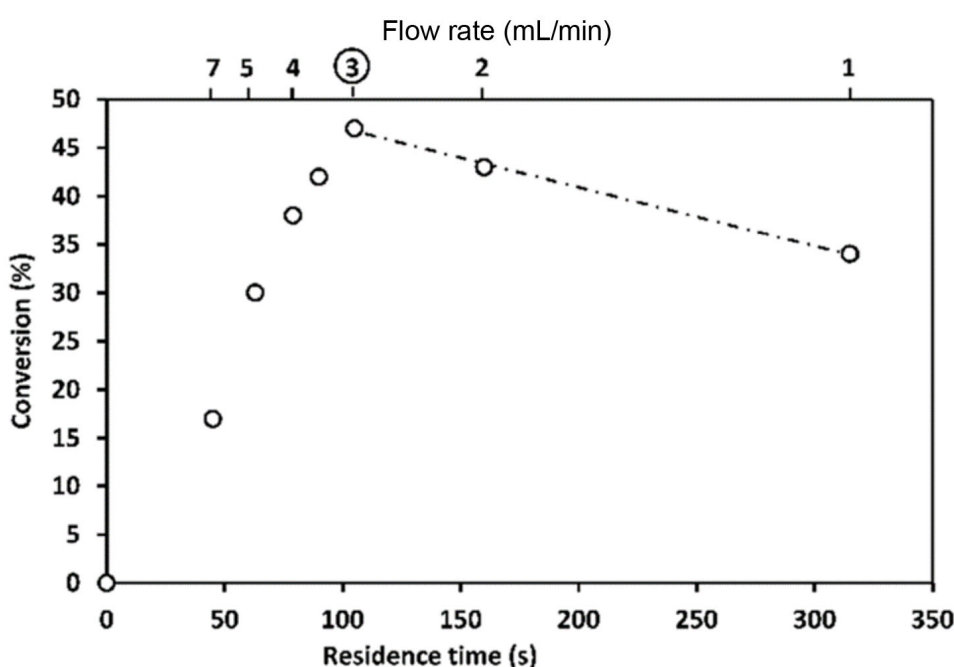


Figure 16. Observation of the change in flow regime during alkylation of benzoic acid by CH_3I in DMF in the presence of DBU in the Low Flow reactor. Reproduced with permission from [159].

An interesting example of dramatic reactivity enhancing upon increase in flow rate (from 0.3 mL/min to 5 mL/min) was reported for in-flow metalation of an acrylate ester containing thiophene moiety with 2,2,6,6-tetramethylpiperidinylmagnesium chloride lithium chloride complex at -25°C . While at low flow rates only low conversions could be achieved with long residence times (5 or 15 min), at high flow rates almost full conversion was achieved within 1 min leading to isolation of the desired product in 72% yield [117].

4. Influence of Residence Time on the Reaction Outcome

The flow rate changes can affect the reaction outcome also by simply changing the residence time (time of contact = time of flowing reagents together without changing the flow rate) without apparent influence of the mixing efficiency. In fact, it may be difficult to separate these effects experimentally.

There are a number of examples when an increase in residence time of reagents leads to an increase in the reaction yield as expected for batch reactions [160]. However, with too long times, selectivity decreases [161] or by-products appear [119]. Special attention should be paid to examples when it is possible to obtain various products in high yields by varying the residence time. A striking example of such an approach is the Br-Li exchange reaction followed by the reaction of the lithiated species with electrophiles performed in flow (Figure 17) [162]. There, kinetically formed 5-substituted product is selectively formed at residence time 0.06 s (yield 84%). Increasing residence time to 63 s gives thermodynamically preferred 3-substituted product in yield 68%. In both cases only traces of another isomer were observed.

The value of the residence time, which is a powerful instrument for controlling reaction outcome, should be optimized as times that are too long may result in a decrease in the product yield probably due to reactants decomposition (Figure 18) [40].

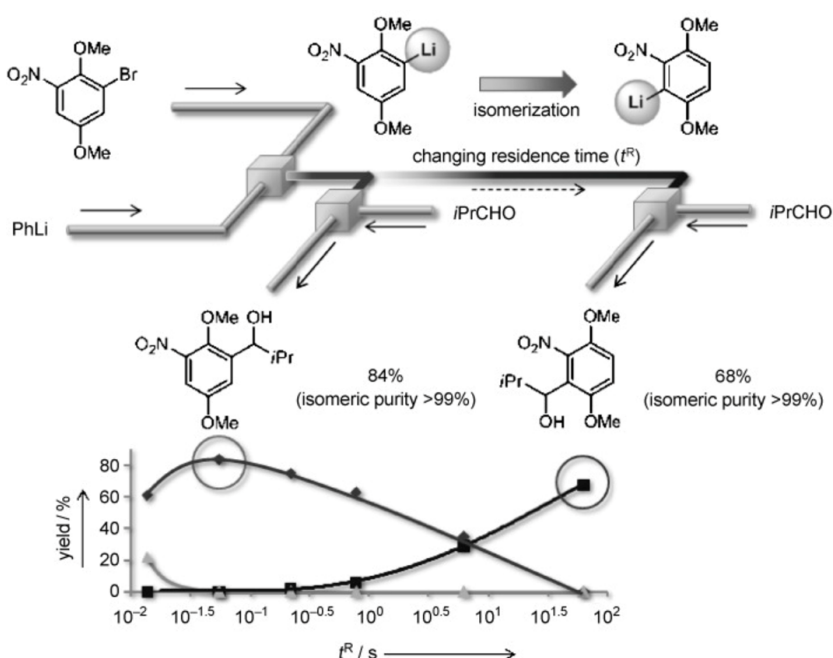


Figure 17. A switch between kinetic and thermodynamic control by changing the residence time of the Br-Li exchange reaction followed by the reaction of the lithiated species with $\text{Pr}^{\text{i}}\text{CHO}$ as electrophile. ◆—5-substituted kinetically formed product, ■—3-substituted thermodynamically preferred product, ▲—initial aromatic reagent. Reproduced with permission from [162]. Copyright © 2009 WILEY-VCH Verlag GmbH & Co. KGaA, Weinheim.

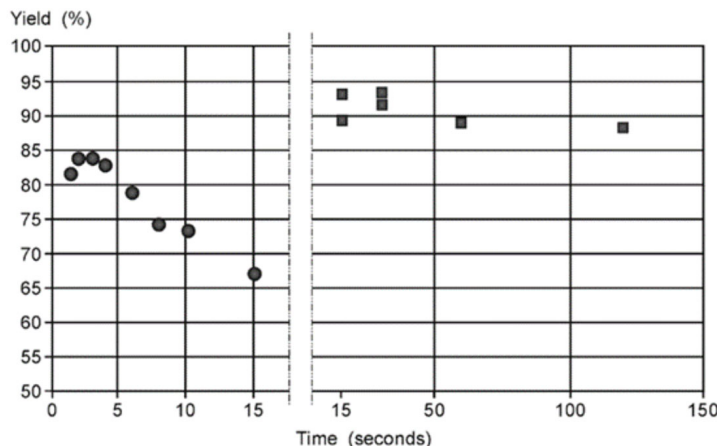


Figure 18. Dependence of the yield on the residence time of the liquid-liquid reaction at 50 °C (●) and 20 °C (■) in the microreactor. Reproduced with permission from [40]. Copyright © 2001 WILEY-VCH Verlag GmbH & Co. KGaA, Weinheim.

5. Conclusions

In conclusion, we demonstrated that variation in flow regime (determined by a combination of mixer design and flow rate) can either improve or worsen the reactivity and lead to completely different products, including stereoisomers. We would like to stress that it is not necessary to homogenize the reaction mixture as much as possible or to mix the reagents with maximum efficiency. The real challenge is to mix reagents the *right way*. To achieve this in a flow reactor one should combine the appropriate values of flow rate and the designs of microreactor.

In terms of the suprameric approach [27], at too high or too low a flow rate (in the particular mixer), the molecules of reagents are incorrectly presented on the surface of supramers, leading to altered stereoselectivity, or form tight supramers (similar to those

discovered recently [113,114,139,158]), in which most of the molecules are located inside the supramer core and are inaccessible for attack, leading to low conversions and yields. The flow rate at which these problems do not exist can be considered optimal.

We can discuss the efficiency of mixing in a similar way. On the one hand, efficiently mixed reagents can react faster and with greater conversion, giving higher yields. On the other hand, the most efficiently mixed system loses the effect of the asymmetry of the supramer surface (since all supramers are disaggregated), which eliminates a possibility of controlling stereoselectivity of the reaction and allows all side processes to proceed.

Chemistry is definitely a statistical science. There are myriads of molecules in the reaction mixture, each of which can react (in one or many ways) or not. For each specific molecule, the reaction proceeds conditionally instantaneously, provided that the reaction partners (who have the fundamental ability to react) have approached the right faces. If it were possible to find a tool or a method of influencing molecules, in which only the approaches we need would be encountered, then product yields and stereoselectivities of any reactions would be high. Experimental data suggest that, for reactions conducted in flow, the flow rate and the design of the microreactor can serve as such tools.

Author Contributions: Conceptualization, I.V.M. and L.O.K.; methodology, I.V.M. and L.O.K.; investigation, I.V.M.; writing—original draft preparation, I.V.M.; writing—review and editing, L.O.K.; visualization, I.V.M. and L.O.K.; supervision, L.O.K.; project administration, L.O.K. All authors have read and agreed to the published version of the manuscript.

Funding: This research received no external funding.

Data Availability Statement: Not applicable.

Conflicts of Interest: The authors declare no conflict of interest.

References

1. Jahnisch, K.; Hessel, V.; Löwe, H.; Baerns, M. Chemistry in microstructured reactors. *Angew. Chem. Int. Ed.* **2004**, *43*, 406. [[CrossRef](#)] [[PubMed](#)]
2. Whitesides, G.M. The origins and the future of microfluidics. *Nature* **2006**, *442*, 368–373. [[CrossRef](#)] [[PubMed](#)]
3. deMello, A.J. Control and detection of chemical reactions in microfluidic systems. *Nature* **2006**, *442*, 394–402. [[CrossRef](#)] [[PubMed](#)]
4. Tanaka, K.; Fukase, K. Acid-mediated reactions under microfluidic conditions: A new strategy for practical synthesis of biofunctional natural products. *Beilstein J. Org. Chem.* **2009**, *5*, 40. [[CrossRef](#)] [[PubMed](#)]
5. Tanaka, K.; Fukase, K. Renaissance of Traditional Organic Reactions under Microfluidic Conditions: A New Paradigm for Natural Products Synthesis. *Org. Process Res. Dev.* **2009**, *13*, 983–990. [[CrossRef](#)]
6. Wegner, J.; Ceylan, S.; Kirschning, A. Ten key issues in modern flow chemistry. *Chem. Commun.* **2011**, *47*, 4583–4592. [[CrossRef](#)] [[PubMed](#)]
7. Hessel, V.; Kralisch, D.; Kockmann, N.; Noël, T.; Wang, Q. Novel Process Windows for Enabling, Accelerating, and Uplifting Flow Chemistry. *ChemSusChem* **2013**, *6*, 746–789. [[CrossRef](#)] [[PubMed](#)]
8. Elvira, K.S.; Casadevall i Solvas, X.; Wootton, R.C.R.; demello, A.J. The past, present and potential for microfluidic reactor technology in chemical synthesis. *Nat. Chem.* **2013**, *5*, 905–915. [[CrossRef](#)]
9. Fukase, K.; Shimoyama, A.; Manabe, Y. Effective Synthesis of Oligosaccharide under Microfluidic Conditions. *J. Synth. Org. Chem. Jpn.* **2015**, *73*, 452–459. [[CrossRef](#)]
10. Fukase, K.; Tanaka, K.; Fujimoto, Y.; Shimoyama, A.; Manabe, Y. Sugar synthesis by microfluidic techniques. In *Glycochemical Synthesis*; Hung, S.-C., Zulueta, M.M.L., Eds.; Wiley Online Books; Wiley: Hoboken, NJ, USA, 2016; pp. 205–219. [[CrossRef](#)]
11. Plutschack, M.B.; Pieber, B.; Gilmore, K.; Seeberger, P.H. The Hitchhiker’s Guide to Flow Chemistry. *Chem. Rev.* **2017**, *117*, 11796–11893. [[CrossRef](#)]
12. Sevim, S.; Sorrenti, A.; Franco, C.; Furukawa, S.; Pané, S.; deMello, A.J.; Puigmartí-Luis, J. Self-assembled materials and supramolecular chemistry within microfluidic environments: From common thermodynamic states to non-equilibrium structures. *Chem. Soc. Rev.* **2018**, *47*, 3788–3803. [[CrossRef](#)] [[PubMed](#)]
13. Guidi, M.; Seeberger, P.H.; Gilmore, K. How to approach flow chemistry. *Chem. Soc. Rev.* **2020**, *49*, 8910–8932. [[CrossRef](#)]
14. Hone, C.A.; Kappe, C.O. Towards the Standardization of Flow Chemistry Protocols for Organic Reactions. *Chem. Methods* **2021**, *1*, 454–467. [[CrossRef](#)]
15. Leslie, A.; Joseph, A.M.; Baumann, M. Functional Group Interconversion Reactions in Continuous Flow Reactors. *Curr. Org. Chem.* **2021**, *25*, 2217–2231. [[CrossRef](#)]
16. Paratore, F.; Bacheva, V.; Bercovici, M.; Kaigala, G.V. Reconfigurable microfluidics. *Nat. Rev. Chem.* **2021**, *6*, 70–80. [[CrossRef](#)] [[PubMed](#)]

17. Burange, A.S.; Osman, S.M.; Luque, R. Understanding flow chemistry for the production of active pharmaceutical ingredients. *iScience* **2022**, *25*, 103892. [CrossRef] [PubMed]
18. Capaldo, L.; Wen, Z.; Noel, T. A field guide to flow chemistry for synthetic organic chemists. *Chem. Sci.* **2023**, *14*, 4230–4247. [CrossRef] [PubMed]
19. Monbaliu, J.-C.M.; Legros, J. Will the next generation of chemical plants be in miniaturized flow reactors? *Lab Chip* **2023**, *23*, 1349–1357. [CrossRef]
20. Numata, M.; Kanzaki, C. Supramolecular Chemistry of a Moving Solution: Flow Drives New Non-covalent Bond Formation. *Chem. Lett.* **2023**, *52*, 602–610. [CrossRef]
21. Ehrfeld, W.; Hessel, V.; Löwe, H. (Eds.) *Micromixers*. In *Microreactors*; Wiley: Hoboken, NJ, USA, 2000; pp. 41–85. [CrossRef]
22. Suryawanshi, P.L.; Gumfekar, S.P.; Bhanvase, B.A.; Sonawane, S.H.; Pimplapure, M.S. A review on microreactors: Reactor fabrication, design, and cutting-edge applications. *Chem. Eng. Sci.* **2018**, *189*, 431–448. [CrossRef]
23. Bojang, A.A.; Wu, H.-S. Design, fundamental principles of fabrication and applications of microreactors. *Processes* **2020**, *8*, 891. [CrossRef]
24. Dong, Z.; Wen, Z.; Zhao, F.; Kuhn, S.; Noel, T. Scale-up of micro- and milli-reactors: An overview of strategies, design principles and applications. *Chem. Eng. Sci. X* **2021**, *10*, 100097. [CrossRef]
25. Kucherov, F.A.; Romashov, L.V.; Ananikov, V.P. Development of 3D + G printing for the design of customizable flow reactors. *Chem. Eng. J.* **2022**, *430*, 132670. [CrossRef]
26. Whitesides, G.M. Whitesides' Group: Writing a Paper. *Adv. Mater.* **2004**, *16*, 1375–1377. [CrossRef]
27. Kononov, L.O. Chemical reactivity and solution structure: On the way to a paradigm shift? *RSC Adv.* **2015**, *5*, 46718–46734. [CrossRef]
28. Reynolds, O. XXIX. An experimental investigation of the circumstances which determine whether the motion of water shall be direct or sinuous, and of the law of resistance in parallel channels. *Philos. Trans. R. Soc. Lond.* **1883**, *174*, 935–982. [CrossRef]
29. Nguyen, N.-T.; Wu, Z. Micromixers—A review. *J. Micromech. Microeng.* **2005**, *15*, R1–R16. [CrossRef]
30. Hisamoto, H.; Saito, T.; Tokeshi, M.; Hibara, A.; Kitamori, T. Fast and high conversion phase-transfer synthesis exploiting the liquid–liquid interface formed in a microchannel chip. *Chem. Commun.* **2001**, 2662–2663. [CrossRef]
31. Ottino, J.M. Mixing, Chaotic Advection, and Turbulence. *Annu. Rev. Fluid Mech.* **1990**, *22*, 207–254. [CrossRef]
32. Ottino, J.M. Mixing and chemical reactions a tutorial. *Chem. Eng. Sci.* **1994**, *49*, 4005–4027. [CrossRef]
33. Baldyga, J.; Bourne, J.R. *Turbulent Mixing and Chemical Reactions*; Wiley: Chichester, UK, 1999; p. 896.
34. Bourne, J.R. Mixing and the Selectivity of Chemical Reactions. *Org. Process Res. Dev.* **2003**, *7*, 471–508. [CrossRef]
35. Hessel, V.; Löwe, H.; Schönfeld, F. Micromixers—A review on passive and active mixing principles. *Chem. Eng. Sci.* **2005**, *60*, 2479–2501. [CrossRef]
36. Lee, C.-Y.; Chang, C.-L.; Wang, Y.-N.; Fu, L.-M. Microfluidic Mixing: A Review. *Int. J. Mol. Sci.* **2011**, *12*, 3263–3287. [CrossRef] [PubMed]
37. Ghanem, A.; Lemenand, T.; Della Valle, D.; Peerhossaini, H. Static mixers: Mechanisms, applications, and characterization methods—A review. *Chem. Eng. Res. Des.* **2014**, *92*, 205–228. [CrossRef]
38. Arimond, J.; Erwin, L. A simulation of a motionless mixer. *Chem. Eng. Commun.* **1985**, *37*, 105–126. [CrossRef]
39. Ehrfeld, W.; Golbig, K.; Hessel, V.; Löwe, H.; Richter, T. Characterization of Mixing in Micromixers by a Test Reaction: Single Mixing Units and Mixer Arrays. *Ind. Eng. Chem. Res.* **1999**, *38*, 1075–1082. [CrossRef]
40. Wörz, O.; Jäckel, K.P.; Richter, T.; Wolf, A. Microreactors—A New Efficient Tool for Reactor Development. *Chem. Eng. Technol.* **2001**, *24*, 138–142. [CrossRef]
41. Johnson, T.J.; Ross, D.; Locascio, L.E. Rapid Microfluidic Mixing. *Anal. Chem.* **2002**, *74*, 45–51. [CrossRef]
42. Stroock, A.D.; Dertinger, S.K.W.; Ajdari, A.; Mezić, I.; Stone, H.A.; Whitesides, G.M. Chaotic Mixer for Microchannels. *Science* **2002**, *295*, 647–651. [CrossRef]
43. Engler, M.; Kockmann, N.; Kiefer, T.; Woias, P. Numerical and experimental investigations on liquid mixing in static micromixers. *Chem. Eng. J.* **2004**, *101*, 315–322. [CrossRef]
44. Kockmann, N.; Engler, M.; Woias, P. Theoretische und experimentelle Untersuchungen der Mischvorgänge in T-förmigen Mikroreaktoren—Teil 3: Konvektives Mischen und chemische Reaktionen. *Chem. Ing. Tech.* **2004**, *76*, 1777–1783. [CrossRef]
45. Mae, K.; Maki, T.; Hasegawa, I.; Eto, U.; Mizutani, Y.; Honda, N. Development of a new micromixer based on split/recombination for mass production and its application to soap free emulsifier. *Chem. Eng. J.* **2004**, *101*, 31–38. [CrossRef]
46. Bothe, D.; Stemich, C.; Warnecke, H.-J. Fluid mixing in a T-shaped micro-mixer. *Chem. Eng. Sci.* **2006**, *61*, 2950–2958. [CrossRef]
47. Hardt, S.; Pennemann, H.; Schönfeld, F. Theoretical and experimental characterization of a low-Reynolds number split-and-recombine mixer. *Microfluid. Nanofluid.* **2006**, *2*, 237–248. [CrossRef]
48. Kockmann, N.; Kiefer, T.; Engler, M.; Woias, P. Convective mixing and chemical reactions in microchannels with high flow rates. *Sens. Actuators B* **2006**, *117*, 495–508. [CrossRef]
49. Kockmann, N.; Dreher, S.; Woias, P. Unsteady Laminar Flow Regimes and Mixing in T-Shaped Micromixers. In Proceedings of the ASME 2007 5th International Conference on Nanochannels, Microchannels, and Minichannels, Puebla, Mexico, 18–20 June 2007; ASME: Puebla, Mexico, 2007; pp. 671–678. [CrossRef]
50. Kockmann, N. *Transport Phenomena in Micro Process Engineering*, 1st ed.; Springer: Berlin/Heidelberg, Germany, 2008; p. 365. [CrossRef]

51. Fang, W.-F.; Yang, J.-T. A novel microreactor with 3D rotating flow to boost fluid reaction and mixing of viscous fluids. *Sens. Actuators B* **2009**, *140*, 629–642. [[CrossRef](#)]
52. Singh, M.K.; Anderson, P.D.; Meijer, H.E.H. Understanding and Optimizing the SMX Static Mixer. *Macromol. Rapid Commun.* **2009**, *30*, 362–376. [[CrossRef](#)]
53. Dreher, S.; Engler, M.; Kockmann, N.; Woias, P. Theoretical and Experimental Investigations of Convective Micromixers and Microreactors for Chemical Reactions. In *Micro and Macro Mixing: Analysis, Simulation and Numerical Calculation*; Bockhorn, H., Mewes, D., Peukert, W., Warnecke, H.-J., Eds.; Springer: Berlin/Heidelberg, Germany, 2010; pp. 325–346. [[CrossRef](#)]
54. Suh, Y.K.; Kang, S. A Review on Mixing in Microfluidics. *Micromachines* **2010**, *1*, 82–111. [[CrossRef](#)]
55. Kockmann, N.; Roberge, D.M. Scale-up concept for modular microstructured reactors based on mixing, heat transfer, and reactor safety. *Chem. Eng. Process.* **2011**, *50*, 1017–1026. [[CrossRef](#)]
56. Zhdanov, V.; Chorny, A. Development of macro- and micromixing in confined flows of reactive fluids. *Int. J. Heat Mass Transf.* **2011**, *54*, 3245–3255. [[CrossRef](#)]
57. Schwolow, S.; Hollmann, J.; Schenkel, B.; Roeder, T. Application-Oriented Analysis of Mixing Performance in Microreactors. *Org. Process Res. Dev.* **2012**, *16*, 1513–1522. [[CrossRef](#)]
58. Orsi, G.; Roudgar, M.; Brunazzi, E.; Galletti, C.; Mauri, R. Water–ethanol mixing in T-shaped microdevices. *Chem. Eng. Sci.* **2013**, *95*, 174–183. [[CrossRef](#)]
59. Wunderlich, B.; Nettels, D.; Benke, S.; Clark, J.; Weidner, S.; Hofmann, H.; Pfeil, S.H.; Schuler, B. Microfluidic mixer designed for performing single-molecule kinetics with confocal detection on timescales from milliseconds to minutes. *Nat. Protoc.* **2013**, *8*, 1459–1474. [[CrossRef](#)] [[PubMed](#)]
60. Liu, Z.; Guo, L.; Huang, T.; Wen, L.; Chen, J. Experimental and CFD studies on the intensified micromixing performance of micro-impinging stream reactors built from commercial T-junctions. *Chem. Eng. Sci.* **2014**, *119*, 124–133. [[CrossRef](#)]
61. Woitalka, A.; Kuhn, S.; Jensen, K.F. Scalability of mass transfer in liquid–liquid flow. *Chem. Eng. Sci.* **2014**, *116*, 1–8. [[CrossRef](#)]
62. Ghotli, R.A.; Abdul Aziz, A.R.; Ibrahim, S. Liquid–liquid mass transfer studies in various stirred vessel designs. *Rev. Chem. Eng.* **2015**, *31*, 329–343. [[CrossRef](#)]
63. Jasińska, M. Test Reactions to Study Efficiency of Mixing. *Chem. Eng. Process.* **2015**, *36*, 171–208. [[CrossRef](#)]
64. Wu, K.-J.; Nappo, V.; Kuhn, S. Hydrodynamic Study of Single- and Two-Phase Flow in an Advanced-Flow Reactor. *Ind. Eng. Chem. Res.* **2015**, *54*, 7554–7564. [[CrossRef](#)]
65. Luo, J.-Z.; Luo, Y.; Chu, G.-W.; Arowo, M.; Xiang, Y.; Sun, B.-C.; Chen, J.-F. Micromixing efficiency of a novel helical tube reactor: CFD prediction and experimental characterization. *Chem. Eng. Sci.* **2016**, *155*, 386–396. [[CrossRef](#)]
66. Plouffe, P.; Bittel, M.; Sieber, J.; Roberge, D.M.; Macchi, A. On the scale-up of micro-reactors for liquid–liquid reactions. *Chem. Eng. Sci.* **2016**, *143*, 216–225. [[CrossRef](#)]
67. Gobert, S.R.L.; Kuhn, S.; Braeken, L.; Thomassen, L.C.J. Characterization of Milli- and Microflow Reactors: Mixing Efficiency and Residence Time Distribution. *Org. Process Res. Dev.* **2017**, *21*, 531–542. [[CrossRef](#)]
68. Kockmann, N. Transport Phenomena and Chemical Reactions in Modular Microstructured Devices. *Heat Transf. Eng.* **2017**, *38*, 1316–1330. [[CrossRef](#)]
69. Rahimi, M.; Azimi, N.; Parsamogadam, M.A.; Rahimi, A.; Masahy, M.M. Mixing performance of T, Y, and oriented Y-micromixers with spatially arranged outlet channel: Evaluation with Villermaux/Dushman test reaction. *Microsyst. Technol.* **2017**, *23*, 3117–3130. [[CrossRef](#)]
70. Reckamp, J.M.; Bindels, A.; Duffield, S.; Liu, Y.C.; Bradford, E.; Ricci, E.; Susanne, F.; Rutter, A. Mixing Performance Evaluation for Commercially Available Micromixers Using Villermaux-Dushman Reaction Scheme with the Interaction by Exchange with the Mean Model. *Org. Process Res. Dev.* **2017**, *21*, 816–820. [[CrossRef](#)]
71. Zhou, M.; Bai, D.; Zong, Y.; Zhao, L.; Thornock, J.N. Numerical investigation of turbulent reactive mixing in a novel coaxial jet static mixer. *Chem. Eng. Process.* **2017**, *122*, 190–203. [[CrossRef](#)]
72. Ansari, M.A.; Kim, K.-Y.; Kim, S.M. Numerical and Experimental Study on Mixing Performances of Simple and Vortex Micro T-Mixers. *Micromachines* **2018**, *9*, 204. [[CrossRef](#)]
73. Levesque, F.; Rogus, N.J.; Spencer, G.; Grigorov, P.; McMullen, J.P.; Thaisrivongs, D.A.; Davies, I.W.; Naber, J.R. Advancing Flow Chemistry Portability: A Simplified Approach to Scaling Up Flow Chemistry. *Org. Process Res. Dev.* **2018**, *22*, 1015–1021. [[CrossRef](#)]
74. Mariotti, A.; Galletti, C.; Mauri, R.; Salvetti, M.V.; Brunazzi, E. Steady and unsteady regimes in a T-shaped micro-mixer: Synergic experimental and numerical investigation. *Chem. Eng. J.* **2018**, *341*, 414–431. [[CrossRef](#)]
75. Rossetti, I. Continuous flow (micro-)reactors for heterogeneously catalyzed reactions: Main design and modelling issues. *Catal. Today* **2018**, *308*, 20–31. [[CrossRef](#)]
76. Su, Y.; Song, Y.; Xiang, L. Continuous-Flow Microreactors for Polymer Synthesis: Engineering Principles and Applications. *Top. Curr. Chem.* **2018**, *376*, 44. [[CrossRef](#)]
77. Li, W.; Xia, F.; Qin, H.; Zhang, M.; Li, W.; Zhang, J. Numerical and experimental investigations of micromixing performance and efficiency in a pore-array intensified tube-in-tube microchannel reactor. *Chem. Eng. J.* **2019**, *370*, 1350–1365. [[CrossRef](#)]
78. Wang, J.; Zhang, N.; Chen, J.; Rodgers, V.G.J.; Brisk, P.; Grover, W.H. Finding the optimal design of a passive microfluidic mixer. *Lab Chip* **2019**, *19*, 3618–3627. [[CrossRef](#)] [[PubMed](#)]

79. Camarri, S.; Mariotti, A.; Galletti, C.; Brunazzi, E.; Mauri, R.; Salvetti, M.V. An Overview of Flow Features and Mixing in Micro T and Arrow Mixers. *Ind. Eng. Chem. Res.* **2020**, *59*, 3669–3686. [[CrossRef](#)]
80. Cheng, D.; Chen, F.-E. Experimental and Numerical Studies of the Phase-Transfer-Catalyzed Wittig Reaction in Liquid-Liquid Slug-Flow Microchannels. *Ind. Eng. Chem. Res.* **2020**, *59*, 4397–4410. [[CrossRef](#)]
81. Desir, P.; Chen, T.-Y.; Bracconi, M.; Saha, B.; Maestri, M.; Vlachos, D.G. Experiments and computations of microfluidic liquid-liquid flow patterns. *React. Chem. Eng.* **2020**, *5*, 39–50. [[CrossRef](#)]
82. Hosseini, F.; Rahimi, M. Computational fluid dynamics and experimental investigations on liquid-liquid mass transfer in T-type microchannels with different mixing channel barrier shapes. *Sep. Sci. Technol.* **2020**, *55*, 3502–3516. [[CrossRef](#)]
83. Mariotti, A.; Antognoli, M.; Galletti, C.; Mauri, R.; Salvetti, M.V.; Brunazzi, E. The role of flow features and chemical kinetics on the reaction yield in a T-shaped micro-reactor. *Chem. Eng. J.* **2020**, *396*, 125223. [[CrossRef](#)]
84. Wang, X.; Wang, Y.; Li, F.; Li, L.; Ge, X.; Zhang, S.; Qiu, T. Scale-up of microreactor: Effects of hydrodynamic diameter on liquid-liquid flow and mass transfer. *Chem. Eng. Sci.* **2020**, *226*, 115838. [[CrossRef](#)]
85. Zhang, H.; Kopfmüller, T.; Achermann, R.; Zhang, J.; Teixeira, A.; Shen, Y.; Jensen, K.F. Accessing multidimensional mixing via 3D printing and showerhead micromixer design. *AIChE J.* **2020**, *66*, e16873. [[CrossRef](#)]
86. Gill, K.K.; Gibson, R.; Yiu, K.H.C.; Hester, P.; Reis, N.M. Microcapillary film reactor outperforms single-bore mesocapillary reactors in continuous flow chemical reactions. *Chem. Eng. J.* **2021**, *408*, 127860. [[CrossRef](#)]
87. Manzano Martínez, A.N.; Jansen, R.; Walker, K.; Assirelli, M.; van der Schaaf, J. Experimental and modeling study on meso- and micromixing in the rotor–stator spinning disk reactor. *Chem. Eng. Res. Des.* **2021**, *173*, 279–288. [[CrossRef](#)]
88. Kravtsova, A.Y.; Ianko, P.E.; Kashkarova, M.V.; Bilsky, A.V.; Kravtsov, Y.V.; Naumov, I.V. Conditions of the Effective Mixing in a T-Type Micromixer at Low Reynolds Numbers. In *Processes in GeoMedia—Volume V*; Chaplina, T., Ed.; Springer International Publishing: Cham, Switzerland, 2022; Volume 5, pp. 35–41. [[CrossRef](#)]
89. Trabzon, L.; Karimian, G.; Khosroshahi, A.R.; Güll, B.; Bakhshayesh, A.G.; Kocak, A.F.; Akyıldız, D.; Aldı, Y.E. High-throughput nanoscale liposome formation via electrohydrodynamic-based micromixer. *Phys. Fluids* **2022**, *34*, 102011. [[CrossRef](#)]
90. Jafarpour, A.M.; Khosroshahi, A.R.; Hanifi, M.; Moghanlou, F.S. Experimental study on the performance of a mini-scale Y-type mixer with two liquid metal-enabled pumps. *Phys. Fluids* **2022**, *34*, 112110. [[CrossRef](#)]
91. Chen, Q.; Zhang, M.; Zheng, C.; Li, H. Numerical Simulation of Mixing Characteristics in a Split-and-Recombine Microchannel. *Heat Transf. Eng.* **2023**, *44*, 1563–1577. [[CrossRef](#)]
92. Jiang, J.; Yang, N.; Liu, H.; Tang, J.; Wang, C.; Wang, R.; Yang, X. Modification of Meso-Micromixing Interaction Reaction Model in Continuous Reactors. *Processes* **2023**, *11*, 1576. [[CrossRef](#)]
93. Falk, L.; Commenge, J.M. Performance comparison of micromixers. *Chem. Eng. Sci.* **2010**, *65*, 405–411. [[CrossRef](#)]
94. Rehage, H.; Kind, M. The first Damköhler number and its importance for characterizing the influence of mixing on competitive chemical reactions. *Chem. Eng. Sci.* **2021**, *229*, 116007. [[CrossRef](#)]
95. Chen, Y.T.; Chen, K.H.; Fang, W.F.; Tsai, S.H.; Fang, J.M.; Yang, J.T. Flash synthesis of carbohydrate derivatives in chaotic microreactors. *Chem. Eng. J.* **2011**, *174*, 421–424. [[CrossRef](#)]
96. Chen, Y.-T.; Fang, W.-F.; Liu, Y.-C.; Yang, J.-T. Analysis of chaos and FRET reaction in split-and-recombine microreactors. *Microfluid. Nanofluid.* **2011**, *11*, 339–352. [[CrossRef](#)]
97. Tanaka, K.; Motomatsu, S.; Koyama, K.; Tanaka, S.I.; Fukase, K. Large-scale synthesis of immunoactivating natural product, pristane, by continuous microfluidic dehydration as the key step. *Org. Lett.* **2007**, *9*, 299–302. [[CrossRef](#)]
98. Tanaka, K.; Mori, Y.; Fukase, K. Practical Synthesis of a Man β (1-4)GlcNTroc Fragment via Microfluidic β -Mannosylation. *J. Carbohydr. Chem.* **2009**, *28*, 1–11. [[CrossRef](#)]
99. Uchinashi, Y.; Nagasaki, M.; Zhou, J.; Tanaka, K.; Fukase, K. Reinvestigation of the C5-acetamide sialic acid donor for α -selective sialylation: Practical procedure under microfluidic conditions. *Org. Biomol. Chem.* **2011**, *9*, 7243–7248. [[CrossRef](#)] [[PubMed](#)]
100. Uchinashi, Y.; Tanaka, K.; Manabe, Y.; Fujimoto, Y.; Fukase, K. Practical and Efficient Method for α -Sialylation with an Azide Sialyl Donor Using a Microreactor. *J. Carbohydr. Chem.* **2014**, *33*, 55–67. [[CrossRef](#)]
101. Audiger, L.; Watts, K.; Elmore, S.C.; Robinson, R.I.; Wirth, T. Ritter Reactions in Flow. *ChemSusChem* **2012**, *5*, 257–260. [[CrossRef](#)] [[PubMed](#)]
102. Baker, A.; Graz, M.; Saunders, R.; Evans, G.J.S.; Kaul, S.; Wirth, T. Flow Synthesis of Symmetrical Di- and Trisulfides Using Phase-Transfer Catalysis. *J. Flow Chem.* **2013**, *3*, 118–121. [[CrossRef](#)]
103. Pradipta, A.R.; Tsutsui, A.; Ogura, A.; Hanashima, S.; Yamaguchi, Y.; Kurbangalieva, A.; Tanaka, K. Microfluidic Mixing of Polyamine with Acrolein Enables the Detection of the [4 + 4] Polymerization of Intermediary Unsaturated Imines: The Properties of a Cytotoxic 1,5-Diazacyclooctane Hydrogel. *Synlett* **2014**, *25*, 2442–2446. [[CrossRef](#)]
104. Umezawa, S.; Yoshihiwa, T.; Tokeshi, M.; Shindo, M. Generation of ynlolates via reductive lithiation using flow microreactors. *Tetrahedron Lett.* **2014**, *55*, 1822–1825. [[CrossRef](#)]
105. Matthew, H.; Thomas, W. Safe use of nitromethane for aldol reactions in flow. *J. Flow Chem.* **2016**, *6*, 202–205. [[CrossRef](#)]
106. Nagasaki, M.; Manabe, Y.; Minamoto, N.; Tanaka, K.; Silipo, A.; Molinaro, A.; Fukase, K. Chemical synthesis of a complex-type N-glycan containing a core fucose. *J. Org. Chem.* **2016**, *81*, 10600–10616. [[CrossRef](#)]
107. Ogasawara, S.; Hayashi, Y. Multistep Continuous-Flow Synthesis of (−)-Oseltamivir. *Synthesis* **2017**, *49*, 424–428. [[CrossRef](#)]
108. Ikawa, T.; Masuda, S.; Akai, S. Microflow Fluorinations of Benzyne: Efficient Synthesis of Fluoroaromatic Compounds. *Chem. Pharm. Bull.* **2018**, *66*, 1153–1164. [[CrossRef](#)] [[PubMed](#)]

109. Katayama, S.; Koge, T.; Katsuragi, S.; Akai, S.; Oishi, T. Flow Synthesis of (*R*)- and (*S*)-(E)-1-Iodohexa-1,5-dien-3-ol: Chiral Building Blocks for Natural Product Synthesis. *Chem. Lett.* **2018**, *47*, 1116–1118. [[CrossRef](#)]
110. Myachin, I.V.; Orlova, A.V.; Kononov, L.O. Glycosylation in flow: Effect of the flow rate and type of the mixer. *Russ. Chem. Bull.* **2019**, *68*, 2126–2129. [[CrossRef](#)]
111. Kondo, M.; Wathsala, H.D.P.; Sako, M.; Hanatani, Y.; Ishikawa, K.; Hara, S.; Takaai, T.; Washio, T.; Takizawa, S.; Sasai, H. Exploration of flow reaction conditions using machine-learning for enantioselective organocatalyzed Rauhut–Currier and [3 + 2] annulation sequence. *Chem. Commun.* **2020**, *56*, 1259–1262. [[CrossRef](#)] [[PubMed](#)]
112. Ota, K.; Fukumoto, S.; Iwase, T.; Mizota, I.; Shimizu, M.; Hachiya, I. Umpolung Reactions of α -Tosyloximino Esters in a Flow System. *Synlett* **2020**, *31*, 1930–1936. [[CrossRef](#)]
113. Myachin, I.V.; Mamirgova, Z.Z.; Stepanova, E.V.; Zinin, A.I.; Chizhov, A.O.; Kononov, L.O. Black swan in phase transfer catalysis: Influence of mixing mode on the stereoselectivity of glycosylation. *Eur. J. Org. Chem.* **2022**, *2022*, e202101377. [[CrossRef](#)]
114. Myachin, I.V.; Kononov, L.O. Phase-transfer catalyzed microfluidic glycosylation: A small change in concentration results in a dramatic increase in stereoselectivity. *Catalysts* **2023**, *13*, 313. [[CrossRef](#)]
115. Miller, P.W.; Long, N.J.; De Mello, A.J.; Vilar, R.; Passchier, J.; Gee, A. Rapid formation of amides via carbonylative coupling reactions using a microfluidic device. *Chem. Commun.* **2006**, *546*–548. [[CrossRef](#)]
116. Webb, D.; Jamison, T.F. Diisobutylaluminum Hydride Reductions Revitalized: A Fast, Robust, and Selective Continuous Flow System for Aldehyde Synthesis. *Org. Lett.* **2012**, *14*, 568–571. [[CrossRef](#)]
117. Ganiek, M.A.; Becker, M.R.; Ketels, M.; Knochel, P. Continuous Flow Magnesiation or Zincation of Acrylonitriles, Acrylates, and Nitroolefins. Application to the Synthesis of Butenolides. *Org. Lett.* **2016**, *18*, 828–831. [[CrossRef](#)]
118. Hafner, A.; Meisenbach, M.; Sedelmeier, J. Flow Chemistry on Multigram Scale: Continuous Synthesis of Boronic Acids within 1 s. *Org. Lett.* **2016**, *18*, 3630–3633. [[CrossRef](#)] [[PubMed](#)]
119. Miyagawa, A.; Tomita, R.; Kurimoto, K.; Yamamura, H. Selective deprotection of trityl group on carbohydrate by microflow reaction inhibiting migration of acetyl group. *Synth. Commun.* **2016**, *46*, 556–562. [[CrossRef](#)]
120. Naber, J.R.; Buchwald, S.L. Packed-Bed Reactors for Continuous-Flow C–N Cross-Coupling. *Angew. Chem. Int. Ed.* **2010**, *49*, 9469–9474. [[CrossRef](#)] [[PubMed](#)]
121. Haroun, S.; Sanei, Z.; Jivan, S.; Schaffer, P.; Ruth, T.J.; Li, P.C.H. Continuous-flow synthesis of $[^{11}\text{C}]$ raclopride, a positron emission tomography radiotracer, on a microfluidic chip. *Can. J. Chem.* **2013**, *91*, 326–332. [[CrossRef](#)]
122. Park, C.P.; Kim, D.-P. Dual-Channel Microreactor for Gas–Liquid Syntheses. *J. Am. Chem. Soc.* **2010**, *132*, 10102–10106. [[CrossRef](#)] [[PubMed](#)]
123. Nagaki, A.; Togai, M.; Suga, S.; Aoki, N.; Mae, K.; Yoshida, J.I. Control of extremely fast competitive consecutive reactions using micromixing. Selective Friedel–Crafts aminoalkylation. *J. Am. Chem. Soc.* **2005**, *127*, 11666–11675. [[CrossRef](#)] [[PubMed](#)]
124. Rys, P. Disguised chemical selectivities. *Acc. Chem. Res.* **1976**, *9*, 345–351. [[CrossRef](#)]
125. Roy, R.; Tropper, F.D.; Cao, S.; Kim, J.M. Anomeric Group Transformations Under Phase-Transfer Catalysis. In *Phase-Transfer Catalysis*; Halpern, M., Ed.; ACS Symposium Series; American Chemical Society: Washington, DC, USA, 1997; Volume 659, pp. 163–180. [[CrossRef](#)]
126. Boons, G.J.; Demchenko, A.V. Recent advances in O-sialylation. *Chem. Rev.* **2000**, *100*, 4539–4566. [[CrossRef](#)]
127. De Meo, C.; Jones, B.T. Chapter two—Chemical synthesis of glycosides of N-acetylneurameric acid. *Adv. Carbohydr. Chem. Biochem.* **2018**, *75*, 215–316. [[CrossRef](#)]
128. De Meo, C.; Goeckner, N. 2.07—Synthesis of glycosides of sialic acid. In *Comprehensive Glycoscience*, 2nd ed.; Barchi, J.J., Vidal, S., Eds.; Elsevier: Amsterdam, The Netherlands, 2021; Volume 2, pp. 228–266. [[CrossRef](#)]
129. Sedláček, M. Large-scale supramolecular structure in solutions of low molar mass compounds and mixtures of liquids: I. Light scattering characterization. *J. Phys. Chem. B* **2006**, *110*, 4329–4338. [[CrossRef](#)]
130. Sedláček, M. Large-scale supramolecular structure in solutions of low molar mass compounds and mixtures of liquids: II. Kinetics of the formation and long-time stability. *J. Phys. Chem. B* **2006**, *110*, 4339–4345. [[CrossRef](#)] [[PubMed](#)]
131. Sedláček, M. Large-scale supramolecular structure in solutions of low molar mass compounds and mixtures of liquids. III. Correlation with molecular properties and interactions. *J. Phys. Chem. B* **2006**, *110*, 13976–13984. [[CrossRef](#)] [[PubMed](#)]
132. Sedláček, M.; Rak, D. Large-Scale Inhomogeneities in Solutions of Low Molar Mass Compounds and Mixtures of Liquids: Supramolecular Structures or Nanobubbles? *J. Phys. Chem. B* **2013**, *117*, 2495–2504. [[CrossRef](#)] [[PubMed](#)]
133. Sedláček, M.; Rak, D. On the origin of mesoscale structures in aqueous solutions of tertiary butyl alcohol: The mystery resolved. *J. Phys. Chem. B* **2014**, *118*, 2726–2737. [[CrossRef](#)] [[PubMed](#)]
134. Rak, D.; Ovadová, M.; Sedláček, M. (Non)existence of bulk nanobubbles: The role of ultrasonic cavitation and organic solutes in water. *J. Phys. Chem. Lett.* **2019**, *10*, 4215–4221. [[CrossRef](#)] [[PubMed](#)]
135. Rak, D.; Sedláček, M. On the mesoscale solubility in liquid solutions and mixtures. *J. Phys. Chem. B* **2019**, *123*, 1365–1374. [[CrossRef](#)] [[PubMed](#)]
136. Rak, D.; Sedláček, M. Solvophobicity-Driven Mesoscale Structures: Stabilizer-Free Nanodispersions. *Langmuir* **2023**, *39*, 1515–1528. [[CrossRef](#)] [[PubMed](#)]
137. Subramanian, D.; Anisimov, M.A. Phase behavior and mesoscale solubilization in aqueous solutions of hydrotropes. *Fluid Phase Equilib.* **2014**, *362*, 170–176. [[CrossRef](#)]

138. Zemb, T.; Kunz, W. Weak aggregation: State of the art, expectations and open questions. *Curr. Opin. Colloid Interface Sci.* **2016**, *22*, 113–119. [[CrossRef](#)]
139. Orlova, A.V.; Laptinskaya, T.V.; Malysheva, N.N.; Kononov, L.O. Light scattering in non-aqueous solutions of low-molecular-mass compounds: Application for supramer analysis of reaction solutions. *J. Solution Chem.* **2020**, *49*, 629–644. [[CrossRef](#)]
140. Orlova, A.V.; Kononov, L.O. Polarimetry as a method for studying the structure of aqueous carbohydrate solutions: Correlation with other methods. *RENSIT* **2020**, *12*, 95–106. [[CrossRef](#)]
141. Orlova, A.V.; Ahiadorme, D.A.; Laptinskaya, T.V.; Kononov, L.O. Supramer analysis of 2,3,5-tri-O-benzoyl- α -D-arabinofuranosyl bromide solutions in different solvents: Supramolecular aggregation of solute molecules in 1,2-dichloroethane mediated by halogen bonds. *Russ. Chem. Bull.* **2021**, *70*, 2214–2219. [[CrossRef](#)]
142. Jelley, E.E. Spectral Absorption and Fluorescence of Dyes in the Molecular State. *Nature* **1936**, *138*, 1009–1010. [[CrossRef](#)]
143. Jelley, E.E. Molecular, Nematic and Crystal States of I: I-Diethyl-Cyanine Chloride. *Nature* **1937**, *139*, 631. [[CrossRef](#)]
144. Scheibe, G. Über die Veränderlichkeit der Absorptionsspektren in Lösungen und die Nebenvalenzen als ihre Ursache. *Angew. Chem.* **1937**, *50*, 212–219. [[CrossRef](#)]
145. Mei, J.; Hong, Y.; Lam, J.W.Y.; Qin, A.; Tang, Y.; Tang, B.Z. Aggregation-Induced Emission: The Whole Is More Brilliant than the Parts. *Adv. Mater.* **2014**, *26*, 5429–5479. [[CrossRef](#)] [[PubMed](#)]
146. Dar, N.; Ankri, R. Theoretical Models, Preparation, Characterization and Applications of Cyanine J-Aggregates: A Minireview. *ChemistryOpen* **2022**, *11*, e202200103. [[CrossRef](#)] [[PubMed](#)]
147. Peng, Q.; Shuai, Z. Molecular mechanism of aggregation-induced emission. *Aggregate* **2021**, *2*, e91. [[CrossRef](#)]
148. Ribo, J.M.; El-Hachemi, Z.; Arteaga, O.; Canillas, A.; Crusats, J. Hydrodynamic Effects in Soft-matter Self-assembly: The Case of J-Aggregates of Amphiphilic Porphyrins. *Chem. Rec.* **2017**, *17*, 713–724. [[CrossRef](#)]
149. Maeda, T.; Mori, T.; Ikeshita, M.; Ma, S.C.; Muller, G.; Ariga, K.; Naota, T. Vortex Flow-controlled Circularly Polarized Luminescence of Achiral Pt(II) Complex Aggregates Assembled at the Air-Water Interface. *Small Methods* **2022**, *6*, 2200936. [[CrossRef](#)]
150. Adero, P.O.; Amarasekara, H.; Wen, P.; Bohé, L.; Crich, D. The experimental evidence in support of glycosylation mechanisms at the S_N1–S_N2 interface. *Chem. Rev.* **2018**, *118*, 8242–8284. [[CrossRef](#)] [[PubMed](#)]
151. Crich, D. En route to the transformation of glycoscience: A chemist's perspective on internal and external crossroads in glycochemistry. *J. Am. Chem. Soc.* **2021**, *143*, 17–34. [[CrossRef](#)] [[PubMed](#)]
152. Ötvös, S.B.; Mándity, I.M.; Fülöp, F. Highly efficient 1,4-addition of aldehydes to nitroolefins: Organocatalysis in continuous flow by solid-supported peptidic catalysts. *ChemSusChem* **2012**, *5*, 266–269. [[CrossRef](#)] [[PubMed](#)]
153. Webb, D.; Jamison, T.F. A Continuous Homologation of Esters: An Efficient Telescoped Reduction-Olefination Sequence. *Org. Lett.* **2012**, *14*, 2465–2467. [[CrossRef](#)] [[PubMed](#)]
154. Andreana, P.R.; Crich, D. Guidelines for O-glycoside formation from first principles. *ACS Cent. Sci.* **2021**, *7*, 1454–1462. [[CrossRef](#)] [[PubMed](#)]
155. Ribó, J.M.; Crusats, J.; Sagués, F.; Claret, J.; Rubires, R. Chiral Sign Induction by Vortices During the Formation of Mesophases in Stirred Solutions. *Science* **2001**, *292*, 2063–2066. [[CrossRef](#)] [[PubMed](#)]
156. Crusats, J.; El-Hachemi, Z.; Ribó, J.M. Hydrodynamic effects on chiral induction. *Chem. Soc. Rev.* **2010**, *39*, 569–577. [[CrossRef](#)] [[PubMed](#)]
157. Sang, Y.; Yang, D.; Duan, P.; Liu, M. Towards homochiral supramolecular entities from achiral molecules by vortex mixing-accompanied self-assembly. *Chem. Sci.* **2019**, *10*, 2718–2724. [[CrossRef](#)]
158. Nagornaya, M.O.; Orlova, A.V.; Stepanova, E.V.; Zinin, A.I.; Laptinskaya, T.V.; Kononov, L.O. The use of the novel glycosyl acceptor and supramer analysis in the synthesis of sialyl- α (2-3)-galactose building block. *Carbohydr. Res.* **2018**, *470*, 27–35. [[CrossRef](#)]
159. Penverne, C.; Hazard, B.; Rolando, C.; Penhoat, M. Scale-up Study of Benzoic Acid Alkylation in Flow: From Microflow Capillary Reactor to a Milliflow Reactor. *Org. Process Res. Dev.* **2017**, *21*, 1864–1868. [[CrossRef](#)]
160. Nagaki, A.; Kenmoku, A.; Moriwaki, Y.; Hayashi, A.; Yoshida, J.-i. Cross-Coupling in a Flow Microreactor: Space Integration of Lithiation and Murahashi Coupling. *Angew. Chem. Int. Ed.* **2010**, *49*, 7543–7547. [[CrossRef](#)]
161. Tomida, Y.; Nagaki, A.; Yoshida, J.-i. Asymmetric Carbolithiation of Conjugated Enynes: A Flow Microreactor Enables the Use of Configurationally Unstable Intermediates before They Epimerize. *J. Am. Chem. Soc.* **2011**, *133*, 3744–3747. [[CrossRef](#)]
162. Nagaki, A.; Kim, H.; Yoshida, J.-i. Nitro-Substituted Aryl Lithium Compounds in Microreactor Synthesis: Switch between Kinetic and Thermodynamic Control. *Angew. Chem. Int. Ed.* **2009**, *48*, 8063–8065. [[CrossRef](#)]

Disclaimer/Publisher's Note: The statements, opinions and data contained in all publications are solely those of the individual author(s) and contributor(s) and not of MDPI and/or the editor(s). MDPI and/or the editor(s) disclaim responsibility for any injury to people or property resulting from any ideas, methods, instructions or products referred to in the content.